Received: 5 March 2023 | Revised: 6 December 2023 | Accepted: 8 January 2024

DOI: 10.1002/jev2.12408

RESEARCH ARTICLE

Heat inactivation of foetal bovine serum performed after EV-depletion influences the proteome of cell-derived extracellular vesicles

Ornella Urzì[1,2] | **Markus Bergqvist**[3] | **Cecilia Lässer**[3] | **Marta Moschetti**[1,2] | **Junko Johansson**[1,4] | **Daniele D´Arrigo**[3,5] | **Roger Olofsson Bagge**[1,4] | **Rossella Crescitelli**[1]

[1]Sahlgrenska Center for Cancer Research and Wallenberg Centre for Molecular and Translational Medicine, Department of Surgery, Institute of Clinical Sciences, Sahlgrenska Academy, University of Gothenburg, Gothenburg, Sweden

[2]Department of Biomedicine, Neurosciences and Advanced Diagnostics (Bi.N.D), University of Palermo, Palermo, Italy

[3]Krefting Research Centre, Department of Internal Medicine and Clinical Nutrition, Institute of Medicine, Sahlgrenska Academy, University of Gothenburg, Gothenburg, Sweden

[4]Department of Surgery, Sahlgrenska University Hospital, Region Västra Götaland, Gothenburg, Sweden

[5]Regenerative Medicine Technologies Laboratory, Ente Ospedaliero Cantonale, Bellinzona, Switzerland

Correspondence
Rossella Crescitelli, Sahlgrenska Center for Cancer Research and Wallenberg Centre for Molecular and Translational Medicine, Department of Surgery, Institute of Clinical Sciences, Sahlgrenska Academy, University of Gothenburg, Gothenburg, Sweden. Email: rossella.crescitelli@gu.se

Funding information
Serena Ehrenströms fond för Kräftsjukdomarnas; University of Gothenburg, Sweden; Anna Lisa and Björnssons foundation; Swedish Cancer Foundation; Wilhelm och Martina Lundgrens Vetenskapsfond, Grant/Award Number: 2023-SA-4142; Swedish Research Council; Assar Gabrielsson's Foundation, Grant/Award Number: FB21-113; Knut and Alice Wallenberg Foundation, and the Wallenberg Centre for Molecular and Translational Medicine, University of Gothenburg, Sweden

Abstract

The release of extracellular vesicles (EVs) in cell cultures as well as their molecular cargo can be influenced by cell culture conditions such as the presence of foetal bovine serum (FBS). Although several studies have evaluated the effect of removing FBS-derived EVs by ultracentrifugation (UC), less is known about the influence of FBS heat inactivation (HI) on the cell-derived EVs. To assess this, three protocols based on different combinations of EV depletion by UC and HI were evaluated, including FBS ultracentrifuged but not heat inactivated (no-HI FBS), FBS heat inactivated before EV depletion (HI-before EV-depl FBS), and FBS heat inactivated after EV depletion (HI-after EV-depl FBS). We isolated large (L-EVs) and small EVs (S-EVs) from FBS treated in the three different ways, and we found that the S-EV pellet from HI-after EV-depl FBS was larger than the S-EV pellet from no-HI FBS and HI-before EV-depl FBS. Transmission electron microscopy, protein quantification, and particle number evaluation showed that HI-after EV-depl significantly increased the protein amount of S-EVs but had no significant effect on L-EVs. Consequently, the protein quantity of S-EVs isolated from three cell lines cultured in media supplemented with HI-after EV-depl FBS was significantly increased. Quantitative mass spectrometry analysis of FBS-derived S-EVs showed that the EV protein content was different when FBS was HI after EV depletion compared to EVs isolated from no-HI FBS and HI-before EV-depl FBS. Moreover, we show that several quantified proteins could be ascribed to human origin, thus demonstrating that FBS bovine proteins can mistakenly be attributed to human cell-derived EVs. We conclude that HI of FBS performed after EV depletion results in changes in the proteome, with molecules that co-isolate with EVs and can contaminate EVs when used in subsequent cell cultures. Our recommendation is, therefore, to always perform HI of FBS prior to EV depletion.

KEYWORDS
extracellular vesicles, foetal bovine serum (FBS), EV depletion by ultracentrifugation, FBS heat-inactivation

1 | INTRODUCTION

Extracellular vesicles (EVs) are lipid-enclosed particles released by all cell types into the extracellular space (van Niel et al., 2018). Although EVs were initially considered garbage bags (Harding et al., 1983; Pan & Johnstone, 1983), they now represent one of the most studied mechanisms of cell–cell communication (Yáñez-Mó et al., 2015). EVs can be found in several biological fluids, including, blood, urine, saliva and cerebrospinal fluid (Aqrawi et al., 2017; Caby et al., 2005; Norman et al., 2021; Pisitkun et al., 2004). Based on their size or biogenesis, several subtypes of EVs have been identified such as exosomes, microvesicles and apoptotic bodies (Crescitelli et al., 2013; Herrmann et al., 2021). The existing overlap between different EV subpopulations is still debated by the EV community, but EVs are commonly divided into two major classes based on size, namely small EVs (S-EVs, 30–200 nm) and large EVs (L-EVs, 200–1000 nm) (Crescitelli et al., 2020; Słomka et al., 2018; Yekula et al., 2020). The cargo of EVs consists of proteins, nucleic acids (e.g., DNA and both coding and non-coding RNA) and lipids, and these vary depending on the releasing cell (Doyle & Wang, 2019). The bioactive molecules carried by EVs can enter target cells and modify their phenotype and metabolism (Yáñez-Mó et al., 2015). The EVs derived from cell lines are the most-studied source of EVs (Wang et al., 2021; Xu et al., 2016). However, the culture conditions and especially the use of foetal bovine serum (FBS) may influence the results of using EVs obtained in *in vitro* studies (Théry et al., 2018).

FBS is widely used to supplement culture media because it provides growth factors, amino acids and vitamins and promotes cell growth and adhesion as well as protects cells from stressful conditions (Gstraunthaler, 2003). Although most cells need FBS to grow properly in culture, the use of FBS carries some disadvantages, mainly related to undefined composition (Baker, 2016; Bryan et al., 2011) and ethical concerns (Jochems et al., 2002; Shoffner & Wallace, 1992). Moreover, because FBS can contain microbial contaminants such as mycoplasma, viruses and prion proteins (Jochems et al., 2002) it is usually heat-inactivated at 56°C for 30–60 min before use (Soltis et al., 1979; Triglia & Linscott, 1980). The heat inactivation also inactivates complement activity and thus is a widely used practice, especially for some cell types, such as immune cells, that can be affected by complement activation (Shen et al., 1997; Soltis et al., 1979).

It has been widely demonstrated that FBS contains large amounts of EVs that might influence the results of EV analysis in *in vitro* studies (Thery et al., 2001). Bovine EVs represent an important limit in the use of FBS as a supplement for cell culture media because they can contaminate cell-derived EV samples (Mannerström et al., 2019) and can influence the growth and phenotype of cultured cells (Ochieng et al., 2009; Shelke et al., 2014). For these reasons, when performing EV studies, it is recommended to deplete the EVs from the FBS (Raposo et al., 1996; Théry et al., 2006, 2018). The most commonly used protocol to deplete EVs from FBS is ultracentrifugation (UC), which consists of centrifuging the FBS at 100,000–120,000 × *g* for 1–18 h and then discarding the pellet of bovine-derived EVs (Raposo et al., 1996; Shelke et al., 2014; Thery et al., 2001). Although UC protocols have been optimized in recent years, some studies suggest that UC does not completely eliminate all FBS-derived EVs (Lehrich et al., 2018; Pham et al., 2021; Shelke et al., 2014). This issue has led to the development of new protocols for EV depletion such as ultrafiltration (Kornilov et al., 2018) and polymer-based precipitation (Haghighitalab et al., 2020), which seem promising, although further studies are needed to improve them.

An aspect that has been neglected in the optimization and evaluation of EV-depletion protocols is the heat inactivation procedure. Although some studies have questioned the heat inactivation procedure (Molenaar-de Backer et al., 2021), this practice remains commonly used in many laboratories, and generally authors do not mention if the FBS was heat inactivated in their studies (Pucci et al., 2021; Yin et al., 2020). Even when it is mentioned, the time and temperature of the procedure are often missing (Aswad et al., 2016; Lehrich et al., 2018). We analysed the top 100 publications in Google Scholar searching for "exosomes OR extracellular vesicles AND FBS AND heat inactivation" in which EVs were isolated from cell culture media. Among the 83 publications in which the authors stated to have performed heat inactivation of FBS, in 24 works the cell media was exchanged with serum-free media or media supplemented with commercial Exo-free FBS before EV isolation, which was different from the remaining 59 publications in which heat-inactivated and EV-depleted FBS was added to the cell culture used for EV isolation. Among them, only five publications specified at which step of the FBS EV-depletion protocol they performed the heat inactivation. This highlights that only rarely do authors specify whether they heat inactivate FBS before or after EV depletion.

Because FBS is known to potentially contaminate cell-derived EV samples, the aim of this study was to determine the effect of heat inactivation on EV purity using quantitative mass spectrometry.

2 | METHODS

2.1 | Preparation of EV-depleted FBS and FBS heat inactivation

The FBS purchased from Sigma-Aldrich (St Louis, MO, lot number: 0001638271) was depleted of EVs following three slightly different protocols based on different combinations of UC and heat inactivation. The UC step was an EV depletion step where the undiluted FBS was ultracentrifuged at 118,000 × *g* (Type 45 Ti rotor, 38,800 rpm, Beckman Coulter, Brea, CA) for 18 h at 4°C

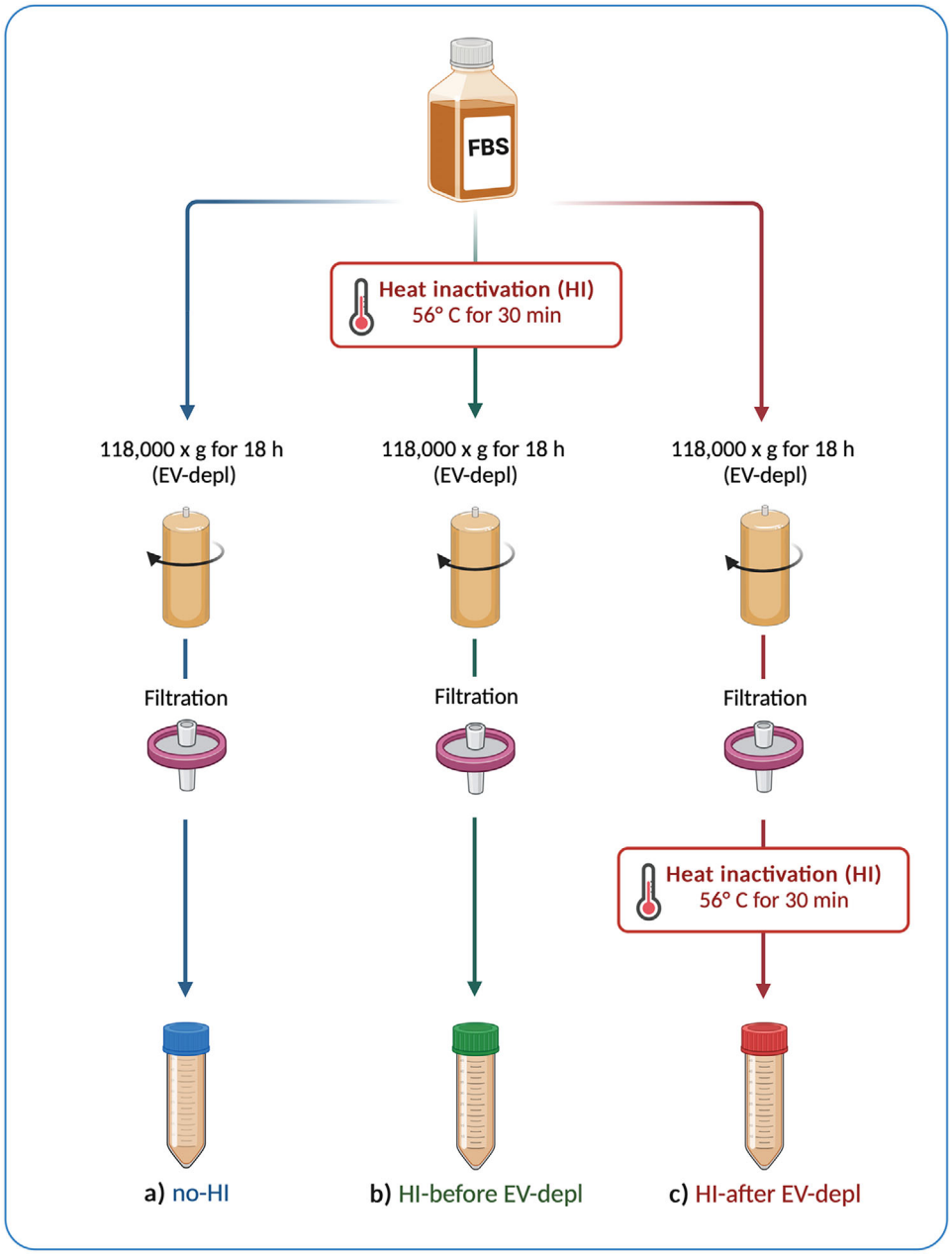

FIGURE 1 Preparation of EV-depleted FBS with three different combinations of UC and heat inactivation. Created with BioRender.com. EV, extracellular vesicles; FBS, foetal bovine serum; UC, ultracentrifugation.

followed by a filtration step (0.22 μm). In the heat inactivation step, the FBS was placed in a water bath at 56°C for 30 min under agitation. Three different combinations of UC and heat inactivation were tested and are described in Figure 1. The protocol was the same for all conditions except for the time when the heat inactivation was performed: (a) FBS was ultracentrifuged but not heat-inactivated at all (no-HI FBS), (b) FBS was heat-inactivated prior to EV depletion (HI-before EV-depl FBS) and (c) FBS was heat inactivated after EV depletion (HI-after EV-depl FBS). For all three conditions the volume of processed FBS was 100 mL. The supernatant was filtered through a 0.22 μm filter to avoid any risk of bacterial contamination and then stored at –20°C until use.

2.2 | Cell cultures

The human skin melanoma cell line MML-1 (CLS, Eppelheim, Germany) and the human uveal melanoma cell lines UM22Bap1$^{+/+}$ and UM22Bap1$^{-/-}$ were used for the isolation of L-EVs and S-EVs. UM22Bap1$^{+/+}$ and UM22Bap1$^{-/-}$ are cell lines isolated from the

liver of a patient affected by uveal melanoma with liver metastasis and a homozygous frameshift deletion in *BAP1*. UM22Bap1$^{+/+}$ cells were transfected using a retroviral vector with a functional copy of *BAP1*, while UM22Bap1$^{-/-}$ cells received an empty control vector (Karlsson et al., 2020). MML-1, UM22Bap1$^{+/+}$ and UM22Bap1$^{-/-}$ cells were cultured in RPMI-1640 (Cytiva, Loga, UT, USA) supplemented with 10% FBS (Sigma-Aldrich), 100 units/ml penicillin, 100 mg/mL streptomycin (Cytiva) and 2 mM L-glutamine (Cytiva). The cells were grown in three different conditions: (a) media supplemented with no-HI FBS, (b) media supplemented with HI-before EV-depl FBS and (c) media supplemented with HI-after EV-depl FBS. Cells were seeded at 50,000 cells/cm^2 and grown in a 37°C humidified incubator with 5% CO_2. Cells were passaged every 3rd day, and cell viability was assessed using the trypan blue exclusion method. Because the cells were constantly grown in EV-depleted medium, no media changes or washing steps were performed prior to EV isolation.

To investigate the contribution of FBS to the S-EV pellet, the RPMI-1640 medium was complemented with 10% of no-HI FBS, HI-before EV-depl FBS or HI-after EV-depl FBS, placed in flasks, and incubated in a 37°C humidified incubator with 5% CO_2 for 72 h to mimic the cell growth conditions. The samples are indicated as "medium + FBS". After 72 h, the medium + FBS samples were used to isolate EVs as described in Section 2.4

2.3 | Cell viability assays and doubling time calculations

In order to assess the viability of the cells grown in the three described conditions, cells from three melanoma cell lines (MML-1, UM22Bap1$^{+/+}$ and UM22Bap1$^{-/-}$) were seeded in flat-bottomed 6-well plates and incubated at 37°C with 5% CO_2 for 72 h. The cell number was determined manually using a trypan blue exclusion assay and an optical microscope, and 5×10^5 cells/well were seeded in complete medium containing FBS processed by one of the three protocols. After 72 h, the cells were photographed using the EVOS XL Core Imaging System (Life Technologies, Bothell, WA, USA). The cells were gently detached from the cell culture plate with 0.25% trypsin at 37°C for approximately 3 min. After washing, one aliquot of each cell line was used for manual counting of the cell number, while the rest of the cells were stained with a Live/Dead Fixable Far Red Dead Cell Stain Kit (Invitrogen, Oregon, US) in phosphate-buffered saline (PBS) and analysed on a BD LSRFortessa instrument (BD Biosciences, San Jose, CA). Subsequent data analysis was performed in BD FACSDiva Software version 9.0.1 (BD Biosciences).

For doubling time calculations, we used the following formulation:

$$Doubling\ time = \frac{\text{Duration} \times \ln(2)}{\ln\left(\frac{\text{Final concentration}}{\text{Initial concentration}}\right)}$$

where the duration was 72 h.

2.4 | Isolation of EVs

Both L-EVs and S-EVs were isolated from three types of samples: the FBS remaining after the EV depletion and heat inactivation (no-HI FBS, HI-before EV-depl FBS, HI-after EV-depl FBS), the medium supplemented with 10% FBS (no-HI FBS, HI-before EV-depl FBS, HI-after EV-depl FBS) but never having been in contact with cells (medium + FBS) and the conditioned media of the MML-1, UM22Bap1$^{+/+}$ and UM22Bap1$^{-/-}$ cell lines. The EV isolation protocol is described in Figure S1, and it was the same for all the samples. Briefly, the FBS/medium + FBS/conditioned medium was collected after 72 h and subjected to differential centrifugations. Cells and debris were removed by centrifugations at 300 × *g* for 10 min and at 2000 × *g* for 20 min at 4°C. The supernatant was centrifuged at 16,500 × *g* for 20 min at 4°C and 118,000 × *g* for 2.5 h at 4°C (Type 45 Ti rotor [Beckman Coulter] at 14,500 rpm and 38,800 rpm and with a k-factor of 1279.1 and 178.6, respectively) to collect L-EVs and S-EVs, respectively. Pellets were resuspended in PBS and stored at −80°C for further experiments.

2.5 | Protein isolation and measurement

The protein concentrations of the L-EVs and S-EVs isolated from FBS, medium + FBS and cell cultures were measured by Qubit (Thermo Fisher Scientific, San Jose, CA) according to the manufacturer's protocol.

2.6 | Nanoparticle tracking analysis (NTA)

The numbers of particles were measured using ZetaView PMX110 (Particle Metrix, Meerbusch, Germany) as described previously (Crescitelli et al., 2020). Measurements were made at all 11 positions, and the camera sensitivity was set to 80 and the shutter

was set to 100. The chamber temperature was automatically measured and integrated into the calculation. Data were analysed using the ZetaView analysis software version 8.2.30.1 with a minimum and maximum size of 5 and 5000 nm, respectively, and a minimum brightness of 20. Three biological replicates were measured from each sample type.

2.7 | Transmission electron microscopy (TEM)

Investigation of EVs by negative staining was performed as previously described (Crescitelli et al., 2021; Svennerholm et al., 2017). Briefly, 5 μg of EVs was placed onto glow discharged 200-mesh formvar/carbon copper grids (Electron Microscopy Sciences, Hatfield Township, PA). The EVs were washed two times with water and then fixed in 2.5% glutaraldehyde. After two further washes in water, the samples were stained with 2% uranyl acetate for 1.5 min. Negative-stained samples were examined on a Talos L120C electron microscope (Thermo Fisher Scientific) at 120 kV with a CCD camera.

2.8 | Sample preparation and digestion for mass spectrometry

The proteomic analysis was performed at The Proteomics Core Facility at Sahlgrenska Academy, Gothenburg University. The samples and reference pools (representative reference material containing equal amounts of all the samples) were digested using a modified filter-aided sample preparation method (Wiśniewski et al., 2009). In short, samples (35 μg) were reduced with 100 mM dithiothreitol at 60°C for 30 min, transferred to Microcon-30kDa Centrifugal Filter Units (Merck) and washed several times with 8 M urea and once with digestion buffer (50 mM triethylammonium bicarbonate, 0.5% sodium deoxycholate) prior to alkylation with 10 mM methyl methanethiosulfonate in digestion buffer for 30 min at RT. Samples were digested with trypsin (Pierce MS-grade Trypsin, Thermo Fisher Scientific, ratio 1:100) at 37°C overnight, and an additional portion of trypsin was added and incubated for another 2 h. Peptides were collected by centrifugation and labelled using tandem mass tag (TMT) 10-plex isobaric mass tagging reagents (Thermo Fisher Scientific) according to the manufacturer's instructions. The samples were combined into one TMT set, and sodium deoxycholate was removed by acidification with 10% TFA. The TMT set was further purified using High Protein and Peptide Recovery Detergent Removal spin columns and Pierce peptide desalting spin columns (both from Thermo Fischer Scientific) according to the manufacturer's instructions prior to basic reversed-phase chromatography fractionation. Peptide separation was performed using a Dionex Ultimate 3000 UPLC system (Thermo Fischer Scientific) and a reverse-phase XBridge BEH C18 column (3.5 μm, 3.0 mm × 150 mm, Waters Corporation) with a gradient from 3% to 100% acetonitrile in 10 mM ammonium formate at pH 10.00 over 23 min at a flow rate of 400 μL/min. The 40 fractions were concatenated into 20 fractions, dried and reconstituted in 3% acetonitrile and 0.2% formic acid.

2.9 | Nanoscale liquid chromatography coupled to tandem mass spectrometry (LC-MS/MS) analysis and database searching

Each fraction was analysed on an Orbitrap Lumos Tribrid mass spectrometer equipped with the FAIMS Pro ion mobility system interfaced with an nLC 1200 liquid chromatography system (all from Thermo Fisher Scientific). Peptides were trapped on an Acclaim Pepmap 100 C18 trap column (100 μm × 2 cm, particle size 5 μm, Thermo Fischer Scientific) and separated on an in-house-constructed analytical column (350 mm × 0.075 mm I.D.) packed with 3 μm Reprosil-Pur C18-AQ particles (Dr. Maisch, Germany) using a gradient from 3% to 80% acetonitrile in 0.2% formic acid over 85 min at a flow rate of 300 nL/min. The FAIMS Pro alternated between the compensation voltages of –40 and –60 V, and essentially the same data-dependent settings were used at both compensation voltages. Precursor ion mass spectra were acquired at 120,000 resolution, a scan range of 450–1375, and a maximum injection time of 50 ms. MS2 analysis was performed in a data-dependent mode, where the most intense doubly or multiply charged precursors were isolated in the quadrupole with a 0.7 m/z isolation window and dynamic exclusion within 10 ppm for 60 s. The isolated precursors were fragmented by collision-induced dissociation at 35% collision energy with a maximum injection time of 50 ms for 3 s ('top speed' setting) and detected in the ion trap. This was followed by multinotch (simultaneous) isolation of the top-10 MS2 fragment ions within the m/z range 400–1200, fragmentation (MS3) by higher-energy collision dissociation at 65% collision energy and detection in the Orbitrap at 50,000 resolution in the m/z range 100–500 and a maximum injection time of 105 ms.

The data files for each set were merged for identification and relative quantification using Proteome Discoverer version 2.4 (Thermo Fisher Scientific). The search was against *Homo sapiens* (Swissprot Database March 2022) and Bovine (Swissprot Database April 2021) using Mascot 2.5 (Matrix Science) as the search engine with a precursor mass tolerance of 5 ppm and a fragment mass tolerance of 0.6 Da. Tryptic peptides were accepted with one missed cleavage, variable modifications of methionine oxidation, and fixed cysteine alkylation, and TMT-labelled modifications of N-termini and lysines were selected. Percolator was used for PSM (peptide spectral match) validation with the strict FDR threshold of 1%. TMT reporter ions were identified

with a 3 mmu mass tolerance in the MS3 higher-energy collision dissociation spectra, and the TMT reporter abundance values for each sample were normalized to the total peptide amount. Only the quantitative results for the unique peptide sequences with a minimum SPS match of 50% and an average S/N above 10 were taken into account for the protein quantification. A reference sample was used as the denominator for calculating the ratios. The quantified proteins were filtered at 1% FDR and grouped by sharing the same sequences in order to minimize redundancy.

In total, 2074 proteins were identified, and 1879 proteins were quantified. Out of the quantified proteins, 870 were assigned to bovines, 893 to humans, 91 both to humans and bovines and 25 were not specified. For the analysis of bovine proteins, the 870 proteins assigned to bovines and the 91 proteins assigned to both humans and bovines were combined to give 961 proteins in total. For the human analysis, we combined the 893 proteins assigned to humans with the 91 proteins assigned to both humans and bovines to give 984 proteins that were used for the analysis. All the quantified proteins are listed in Table S1.

2.10 | Western blot analysis

Both L-EVs and S-EVs isolated from the MML1, BAP1$^{+/+}$ and BAP1$^{-/-}$ cells were analysed by western blot following the MISEV guidelines (Théry et al., 2018). Proteins were isolated from the cell lines using RIPA buffer (Thermo Fisher Scientific) and protease inhibitors (cOmplete, Mini Protease Inhibitor Cocktail, Roche) and were used as a control for the western blot experiments. Cell lysates and cell-derived EVs were loaded on precast 4%–20% polyacrylamide Mini-PROTEAN TGX gels (Bio-Rad Laboratories, Hercules, CA). For validation of the LC-MS/MS data as well as to investigate the presence of bovine proteins in EVs from MML1 cells, 15 μg of S-EVs from FBS and MML1 cells were loaded onto precast 4%–20% polyacrylamide Mini-PROTEAN TGX Stain Free Precast Gels (Bio-Rad Laboratories). The proteins were then transferred to PVDF membranes (Bio-Rad Laboratories) that were incubated with EveryBlot Blocking Buffer (Bio-Rad Laboratories) for 5 min at RT to block unspecific binding. To investigate the EV proteins from the cell lines, we added the following primary antibodies diluted in EveryBlot Blocking Buffer (Bio-Rad Laboratories): anti-Calnexin (1:1.000 dilution, clone C5C9, Cell Signalling Technology, Leiden, The Netherlands), anti-CD63 (1:1.000 dilution, clone H5C6, BD Biosciences, San Jose, CA, non-reducing conditions), anti-Flotillin-1 (1:1000 dilution, clone EPR6041, Abcam, Cambridge, UK) and anti-CD81 (1:1.000 dilution, clone M38, Abcam, non-reducing conditions). For validation of LC-MS/MS data in FBS-derived S-EVs, the primary antibodies anti-HSP90 (1:1000, clone MBH90AB, Thermo Fisher Scientific), anti-HSPA1A (1:200 dilution, clone aa1-641, LSBio, Shirley, MA) and anti-Hba1 (clone aa2-142, 1:200, LSBio) were used. The primary antibodies anti-HSPA1A and anti-Hba1 were used to determine the presence of bovine proteins in EVs from MML1 cells. All of the primary antibodies were diluted in EveryBlot Blocking Buffer (Bio-Rad Laboratories) and were added to the membrane and incubated overnight at +4°C. After three washes, the secondary antibodies diluted in EveryBlot Blocking Buffer (Bio-Rad Laboratories) were added for 1 h at RT. The secondary antibodies were anti-rabbit IgG (horseradish peroxidase conjugated, 1:5.000 dilution, Harlan Sera-Lab, Loughborough, UK) and anti-mouse IgG (horseradish peroxidase conjugated, 1:5.000 dilution, Harlan Sera-Lab). The membranes were finally imaged and analysed with the SuperSignal West Femto maximum sensitivity substrate (Thermo Fisher Scientific) on a ChemiDoc Imaging System (Bio-Rad Laboratories).

2.11 | Enzyme-linked immunosorbent assays (ELISA)

The amount of CPN1 protein was investigated in S-EVs from MML1, BAP$^{1+/+}$ and BAP1$^{-/-}$ cells cultured in no-HI FBS, HI-after EV-depl FBS and HI-before EV-depl FBS using the Bovine Carboxypeptidase N catalytic chain (CPN1) ELISA Kit (BlueGene Biotech, Shanghai, China). Hba1 protein amount in S-EVs isolated from MML1 cells cultured in No-HI FBS, HI-after EV-depl FBS and HI-before EV-depl FBS was determined by the Bovine Hemoglobin A1C (Hba1C) ELISA Kit (MyBioSource, San Diego, CA). All the ELISA assays were performed on 50 μg of S-EVs according to the manufacturers' instructions.

2.12 | Bioinformatics and statistical analysis

Where appropriate, data are expressed as the mean and standard deviation of the mean (SD). Statistical analysis was performed by one-way ANOVA for multiple comparisons in GraphPad Prism 6 (GraphPad Software Inc., La Jolla, CA).

Qlucore Omics Explorer (Qlucore, Lund, Sweden) was used for the principal component analysis. The proteins that were enriched in the HI-after EV-depl FBS group were analysed using the Database for Annotation, Visualization and Integrated Discovery (DAVID; http://david.abcc.ncifcrf.gov/ [accessed: 19–07–2022]) to determine the cellular components associated with these proteins.

2.13 | Data availability

We have submitted all relevant data of our experiments to the EV-TRACK knowledgebase (EV-TRACK ID: EV230994 and EV230995) (Van Deun et al., 2017). The mass spectrometry proteomics data have been deposited to the ProteomeXchange Consortium via the PRIDE (Perez-Riverol et al., 2022) partner repository with the dataset identifier PXD047505 and they have been submitted to Vesiclepedia (Kalra et al., 2012).

3 | RESULTS

3.1 | Heat inactivation of FBS performed after EV-depletion can cause contamination of S-EV pellets

In order to evaluate the possible effects of heat inactivation of FBS on cell-derived EV contamination, the three types of pre-processed FBS (no-HI FBS, HI-before EV-depl FBS, and HI-after EV-depl FBS) were centrifuged to isolate FBS-derived L-EVs and S-EVs as described in Figure S1. The S-EV pellet was clearly visible and had a yellow/brown tint when isolated from HI-after EV-depl FBS, which was different from L-EVs from HI-after EV-depl FBS and the S-EV and L-EV pellets isolated from no-HI FBS and HI-before EV-depl FBS (Figure 2a, left panel). Furthermore, a strong background due to elements surrounding the EVs was visible in TEM images of the S-EVs isolated from HI-after EV-depl FBS. The strong background was not present in images of L-EVs and S-EVs isolated from no-HI FBS or HI-before EV-depl FBS (Figure 2a, right panel). The background was likely due to protein contaminants as demonstrated by the higher amount of protein in these samples compared to the other samples (Figure 2b). While the number of particles did not change significantly among the analysed conditions (Figure S2a), the ratio between the number of particles and amount of proteins in S-EVs isolated from HI-after EV-depl FBS was lower compared to no-HI FBS and HI-before EV-depl FBS indicating the reduced purity of this pellet compared to the other pellets (Figure S2b).

Taking into account that FBS is usually diluted in cell growth media, we also isolated EVs from media supplemented with 10% no-HI FBS, HI-before EV-depl FBS and HI-after EV-depl FBS, but without ever being in contact with the cells (Medium + FBS, Figure S1). Interestingly, the results were consistent with previous observations, and the S-EV pellet of media mixed with HI-after EV-depl FBS resulted in high background when S-EVs were observed by TEM (Figure 3a). In addition, S-EVs obtained from media supplemented with HI-after EV-depl FBS were enriched in contaminants as shown by high levels of proteins in the S-EV pellet isolated from media supplemented with HI-after EV-depl FBS (Figure 3b). The number of particles in S-EVs isolated from media plus HI-after EV-depl FBS was significantly higher compared to S-EVs from no-HI FBS and HI-before EV-depl FBS (Figure S2c). Finally, the purity of S-EVs from media supplemented with HI-after EV-depl FBS was lower compared to S-EVs isolated from media containing no-HI FBS and HI-before EV-depl FBS (Figure S2d). Together, these results show that heat inactivation of FBS induces the production of protein contaminants that may affect the purity of cell-derived S-EV samples if the heat inactivation is performed after EV depletion by UC.

3.2 | FBS heat inactivation performed after EV depletion reduces the purity of S-EVs isolated from cell cultures

To investigate the contribution of FBS to cell-derived EVs, we cultured three melanoma cell lines, MML-1, UM22Bap1$^{+/+}$ and UM22Bap1$^{-/-}$, in media supplemented with no-HI FBS, HI-before EV-depl FBS or HI-after EV-depl FBS. Because several cell culture parameters can affect EV release (Théry et al., 2018), we first confirmed that cell morphology and confluence were not altered when the cells were grown in media containing no-HI no-EV-depl FBS or HI no-EV-depl FBS as well as in all three other culture conditions investigated (no-HI FBS, HI-before EV-depl FBS and HI-after EV-depl FBS) (Figure S3). Moreover, cell viability was evaluated at seeding time (time 0) and after 72 h (when the cell supernatant was harvested to collect EVs) using trypan blue, and the number of live cells was analysed by flow cytometry. The cell viability was similar in all the experimental conditions for the three cell lines, suggesting that the different combinations of EV depletion and heat inactivation did not affect cell viability (Figure S4a–c). Similarly, the doubling time was comparable in media supplemented with no-HI FBS, HI-before EV-depl FBS and HI-after EV-depl FBS in all three cell lines as well as in media with no-HI no-EV-depl FBS and HI no-EV-depl FBS (Figure S4d–f). Overall, these results demonstrated that media supplemented with no-HI FBS, HI-before EV-depl FBS and HI-after EV-depl FBS did not affect the morphology or growth of the MML-1, UM22Bap1$^{+/+}$ and UM22Bap1$^{-/-}$ cell lines.

We next isolated and characterized EVs released by the three different cell lines maintained in the three different culture conditions. The three melanoma cell lines were seeded in media supplemented with no-HI FBS, HI-before EV-depl FBS and HI-after EV-depl FBS, and after 72 h, the L-EVs and S-EVs were isolated (Conditioned medium, Figure S1). Using western blot analysis, we confirmed the EV nature of the samples obtained from the three melanoma cell lines. As suggested by the MISEV

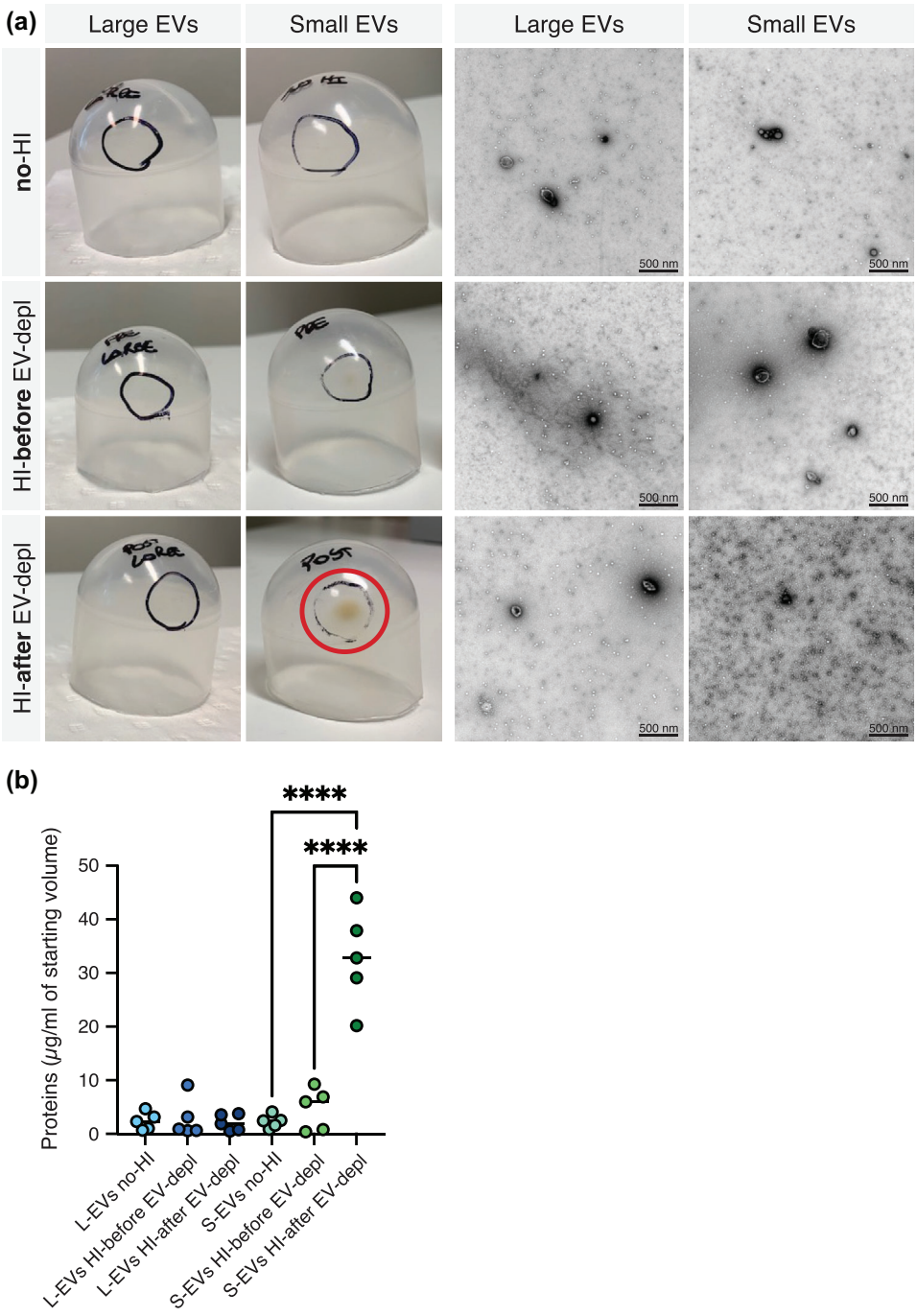

FIGURE 2 Analysis of L-EVs and S-EVs isolated by the differential centrifugation of no-HI FBS, HI-before EV-depl FBS, and HI-after EV-depl FBS. (a, left panel) Representative pictures of pellets obtained by the UC of no-HI FBS, HI-before EV-depl FBS, and HI-after EV-depl FBS. An obviously visible pellet isolated from HI-after EV-depl FBS is indicated (red circle). (a, right panel) TEM images of L-EVs and S-EVs isolated from no-HI FBS, HI-before EV-depl FBS, and HI-after EV-depl FBS. (b) Protein concentrations of L-EVs and S-EVs isolated from no-HI FBS, HI-before EV-depl FBS, and HI-after EV-depl FBS. The results are presented as the mean, but individual values from five different experiments are shown. $N = 5$. ****$p \leq 0.0001$. Statistical significance was calculated by comparing the average values of S-EV samples using one-way ANOVA. EV, extracellular vesicles; EV-depl, EV depleted; FBS, foetal bovine serum; HI, heat inactivation; L-EVs, large EVs S-EVs, small EVs; UC, ultracentrifugation.

guidelines (Théry et al., 2018), three typical EV markers (Flotillin, CD63 and CD81) and a non-EV marker Calnexin (an ER marker) were tested in the EV pellets. Both EV subtypes from all three cell lines were positive for the EV markers and negative for the non-EV marker (Figure S5). The presence of EVs was confirmed by TEM, and both L-EVs and S-EVs showed typical morphology in all conditions analysed (Figure 4a and Figure S6a,b). Of note, elements surrounding the S-EVs (a strong image background) were visible in TEM images of S-EVs isolated from cells grown in media supplemented with HI-after EV-depl FBS

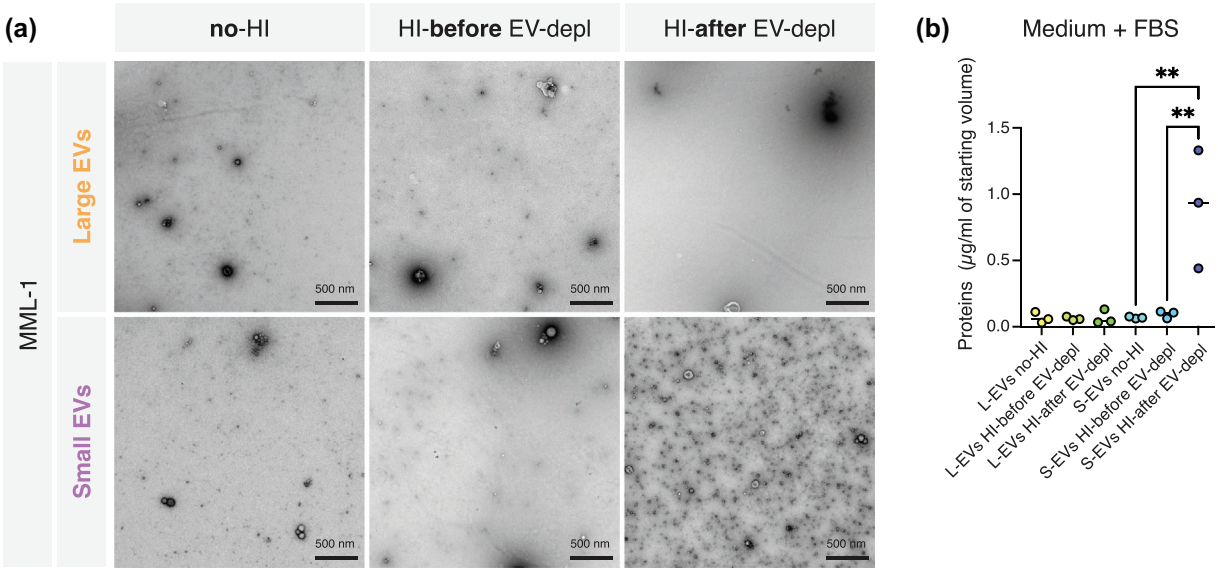

FIGURE 3 Analysis of pellets obtained by the differential centrifugation of media supplemented with no-HI FBS, HI-before EV-depl FBS, and HI-after EV-depl FBS. (a) TEM images of L-EVs and S-EVs isolated from media supplemented with no-HI FBS, HI-before EV-depl FBS, and HI-after EV-depl FBS. (b) Protein concentrations of L-EVs and S-EVs isolated from media supplemented with no-HI FBS, HI-before EV-depl FBS, and HI-after EV-depl FBS. The results are presented as the mean, but individual values from three different experiments are shown. $N = 3$. $^{**}p \leq 0.01$. Statistical significance was calculated by comparing the average values of S-EV samples using one-way ANOVA. EV, extracellular vesicles; EV-depl, EV depleted; FBS, foetal bovine serum; HI, heat inactivation; L-EVs, large EVs; S-EVs, small EVs; TEM, transmission electron microscopy.

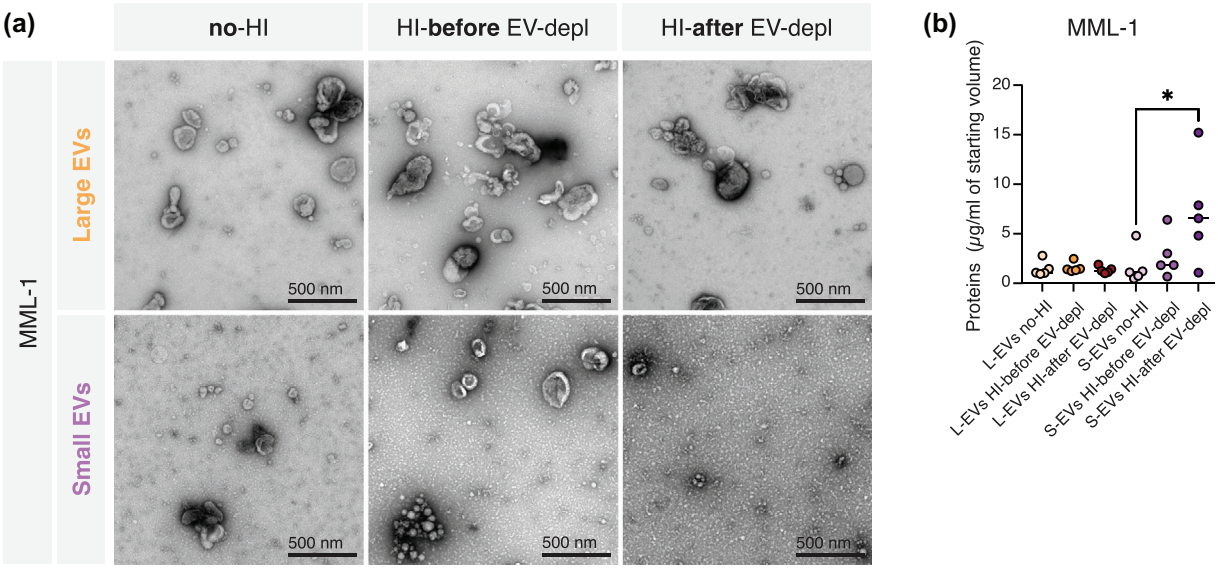

FIGURE 4 Analysis of EVs isolated from MML-1 cells cultured in media supplemented with no-HI FBS, HI-before EV-depl FBS, and HI-after EV-depl FBS. (a) TEM analysis of EVs isolated from MML-1 cells cultured in media supplemented with no-HI FBS, HI-before EV-depl FBS, and HI-after EV-depl FBS. (b) Protein concentrations of L-EVs and S-EVs isolated from MML-1 cells in media supplemented with no-HI FBS, HI-before EV-depl FBS, and HI-after EV-depl FBS. The results are presented as the mean, but individual values from five different experiments are shown. $N = 5$. $^{*}p \leq 0.05$. Statistical significance was calculated by comparing the average values of S-EV samples using one-way ANOVA. EV, extracellular vesicles; EV-depl, EV depleted; FBS, foetal bovine serum; HI, heat inactivation; L-EVs, large EVs; S-EVs, small EVs; TEM, transmission electron microscopy.

but not in TEM images of S-EVs isolated from cells grown in media supplemented with no-HI FBS or HI-before EV-depl FBS (Figure 4a and Figure S6a,b). The amount of protein in cell-derived S-EVs was significantly higher when cells were cultured in media supplemented with HI-after EV-depl FBS compared to no-HI FBS and HI-before EV-depl FBS (Figure 4b, Figure S6c,d). Although we did not observe any significant changes among the different conditions in the number of particles isolated from the three cell lines (Figure S7a,c,e), the ratio between the number of particles and the amount of protein was lower in HI-after

EV-depl FBS than no-HI FBS or HI-before EV-depl FBS samples due to the large amount of proteins (Figure S7b,d,f). Together, these results suggest that the increase in proteins identified in FBS when heat inactivation was performed after EV depletion (Figures 2 and 3) reduced the purity of S-EVs isolated from cell cultures.

3.3 | Quantitative proteomic analysis revealed that heat inactivation performed after EV depletion influences the FBS-derived S-EV proteome

To further investigate the nature of the contaminants induced by the heat inactivation process, we performed quantitative proteomics on S-EV pellets isolated from FBS previously treated in the three different conditions (as described in Figure 1 and in Figure S1). A total of 961 bovine proteins were quantified. A principal component analysis including all quantified bovine proteins was performed to visualize the relationship between the S-EV pellets isolated under the three different conditions. Component 1, representing the largest variability with 53%, distinguished the HI-after EV-depl FBS-derived S-EVs from the no-HI FBS-derived S-EVs and HI-before EV-depl FBS-derived S-EVs, indicating that the pellet isolated from HI-after EV-depl FBS was different from the pellets isolated from no-HI FBS and HI-before EV-depl FBS (Figure 5a). Proteins quantified in S-EVs from no-HI FBS and HI-before EV-depl FBS were similar as shown by volcano plot analysis (Figure 5b, Table S2). However, proteins quantified in S-EVs from HI-after EV-depl FBS were significantly different from the proteins quantified in S-EVs from no-HI FBS. In particular, 268 and 32 proteins were enriched and decreased, respectively, in the HI-after EV-depl FBS group compared to the no-HI FBS group (Figure 5c1, Table S3). The top 20 enriched and decreased proteins in HI-after EV-depl FBS-derived S-EVs versus the no-HI FBS group are shown in Figure 5c2 and Figure 5c3, respectively. Proteins quantified in S-EVs from HI-after EV-depl FBS were also different from the proteins quantified in HI-before EV-depl FBS. In particular, 62 proteins were enriched and 16 were decreased in HI-after EV-depl FBS compared to HI-before EV-depl FBS (Figure 5d1, Table S4). The top 20 proteins enriched in HI-after EV-depl FBS versus HI-after EV-depl FBS are shown in Figure 5d2, while the top 20 decreased proteins in HI-after EV-depl FBS versus HI-before EV-depl FBS are shown in Figure 5d3.

HSP90, HSPA1A and Hba1 were among the enriched proteins in S-EVs from HI-after EV-depl FBS versus no-HI FBS-derived S-EVs (Table S3). To validate this, western blot analysis of HSP90, HSPA1A and Hba1 in S-EVs isolated from no-HI FBS, HI-before EV-depl FBS and HI-after EV-depl FBS was performed. The results showed strong enrichment for all three proteins in the S-EVs isolated from HI-after EV-depl FBS as compared to no-HI FBS and HI-before EV-depl FBS (Figure 6a–f). These results suggested that heat inactivation performed after EV depletion by UC influenced the protein content in the FBS.

We next evaluated the contamination of cell-derived S-EVs by proteins of bovine origin, and we performed the western blot analysis using the same antibodies used to validate the proteomics results. In line with the data obtained for FBS-derived S-EVs, we found that bovine HSPA1A and Hba1 were strongly enriched in S-EVs isolated from MML-1 cells cultured in media supplemented with HI-after EV-depl FBS compared to no-HI FBS and HI-before EV-depl FBS (Figure 7a–c). Moreover, using ELISA assays able to specifically identify proteins of bovine origin, we measured the levels of CPN1, which was enriched in S-EVs isolated from cells cultured in HI-after EV-depl FBS group versus the no-HI FBS group, and an increase in bovine CPN1 protein levels was observed in S-EVs isolated from MML-1, UM22Bap1$^{+/+}$ and UM22Bap1$^{-/-}$ cells cultured in media supplemented with HI-before EV-depl FBS and HI-after EV-depl FBS versus no-HI FBS (Figure S8a–c). In addition, according to the western blot results (Figure 7a,c), bovine Hba1 was significantly enriched in S-EVs isolated from MML-1 cells cultured in media supplemented with HI-after EV-depl FBS and HI-before EV-depl FBS compared to no-HI FBS (Figure S8d). These results confirm that FBS-derived proteins can contaminate cell-derived EV samples, especially when the FBS is heat inactivated after EV depletion.

3.4 | Proteins from FBS heat inactivated after EV depletion could be mistakenly attributed to human cell S-EVs

Because the majority of the studies analysing the proteomes of EVs have focused on proteins of human origin, and thus have investigated the human protein list, we also analysed the proteomic results against the human database. A total of 984 proteins were then identified and quantified as human. Principal component analysis was performed including all quantified proteins matched with the human database (Figure 8a). Component 1 represented the largest variability (47%) and distinguished S-EVs obtained from HI-after EV-depl FBS from those obtained from no-HI FBS and HI-before EV-depl FBS. A strong similarity was observed in proteins of S-EVs from no-HI FBS and HI-before EV-depl FBS (Figure 8b, Table S5). In contrast, the proteins in S-EVs from HI-after EV-depl FBS showed significant differences compared to S-EVs from no-HI FBS (Figure 8c1, Table S6). The top 20 enriched proteins in S-EVs from HI-after EV-depl FBS versus no-HI FBS are shown in Figure 8c2, while the top 20 decreased proteins are shown in Figure 8c3. The proteins in S-EVs from HI-after EV-depl FBS also showed significant differences compared to S-EVs from HI-before EV-depl FBS (Figure 8d1, Table S7). Figure 8d2 shows the top 20 enriched proteins in S-EVs from HI-after EV-depl FBS versus HI-before EV-depl FBS, while Figure 8d3 shows the top 20 decreased proteins.

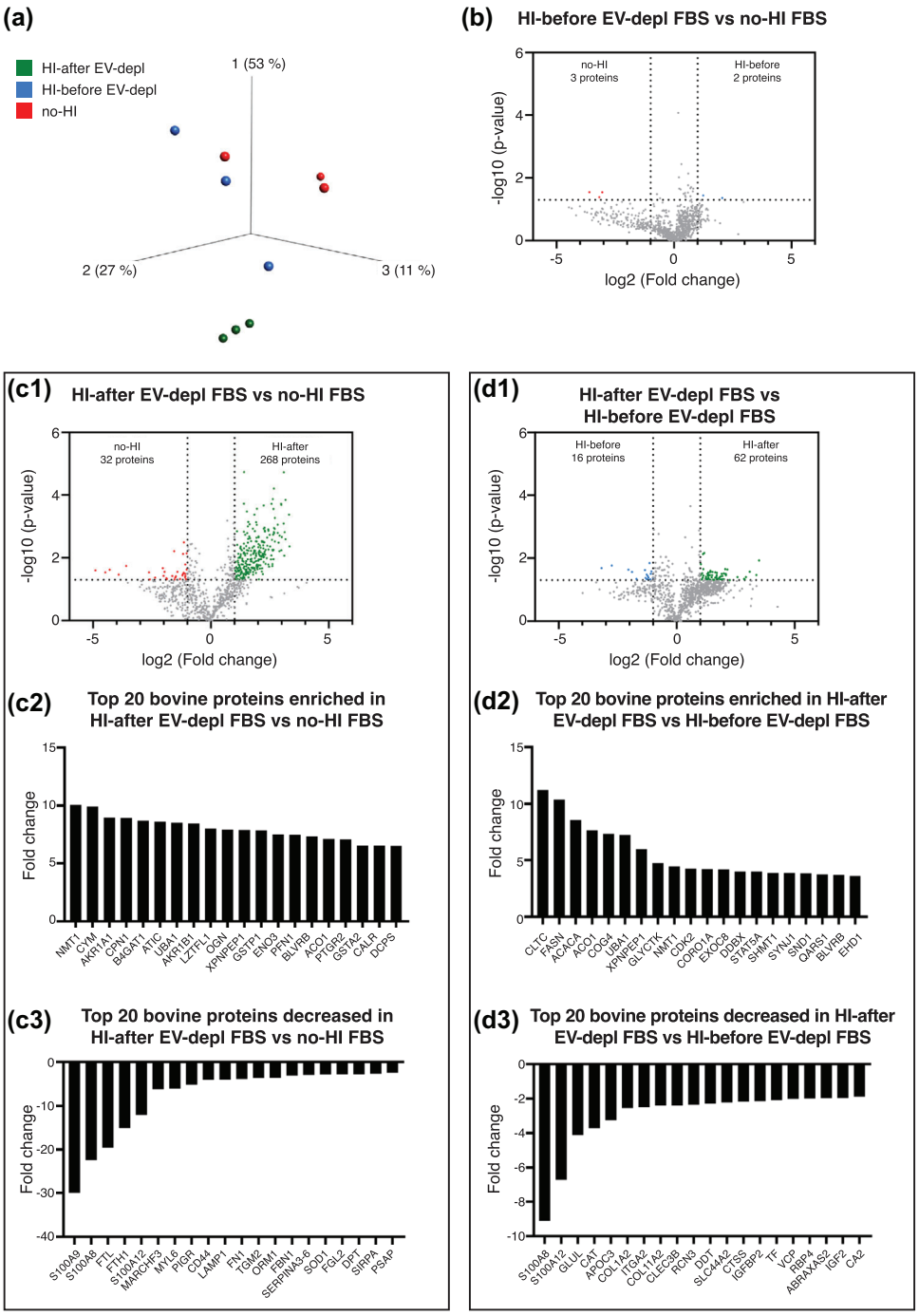

FIGURE 5 Analysis of S-EVs isolated from FBS compared to the bovine dataset. Quantitative proteomics (TMT) was used to determine the differences in the S-EVs isolated from no-HI FBS, HI-before EV-depl FBS, and HI-after EV-depl FBS, $N = 3$. (a) Principal component analysis illustrating the relation between S-EVs isolated from no-HI FBS (red), HI-before EV-depl FBS (blue), and HI-after EV-depl FBS (green). (b, c1 and d1) Volcano plots showing proteins with differential expression between S-EVs from no-HI FBS and HI-before EV-depl FBS (b), between S-EVs from HI-after EV-depl FBS and no-HI FBS (c1), and between S-EVs from HI-before EV-depl FBS and HI-after EV-depl FBS (d1). Grey dotted lines show p-value < 0.05 and two-fold change cut-offs. (c2–c3) The 20 most enriched (c2) and decreased (c3) bovine proteins in S-EVs isolated from HI-after EV-depl FBS versus no-HI FBS. (d2–d3) The 20 most enriched and decreased bovine proteins in S-EVs isolated from HI-after EV-depl FBS versus HI-before EV-depl FBS. $N = 3$. EV, extracellular vesicles; EV-depl, EV depleted; FBS, foetal bovine serum; HI, heat inactivation; S-EVs, small EVs.

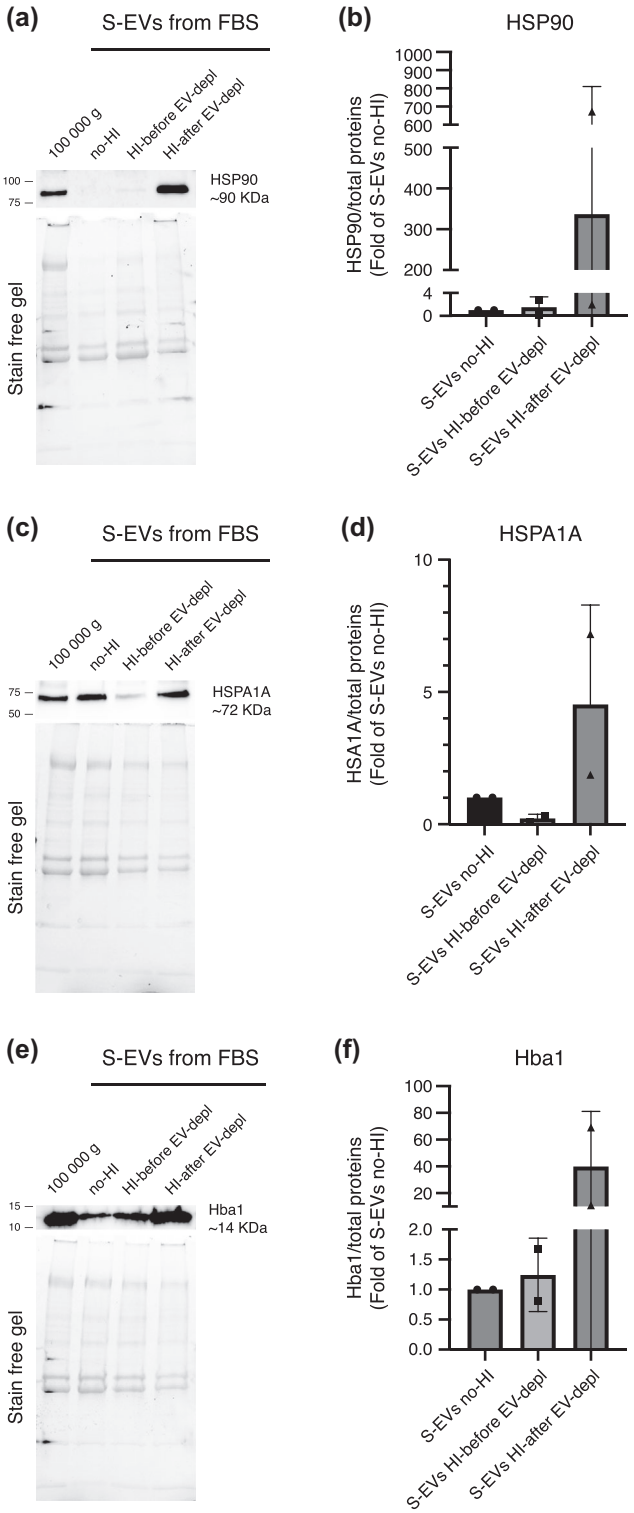

FIGURE 6 Validation of a selection of proteins from the TMT analysis. (a, c, e) Western blot and (b, d, f) densitometric analysis of (a, b) HSP90, (c, d) HSPA1A, and (e, f) Hba1 in S-EVs isolated from no-HI FBS, HI-before EV-depl FBS, and HI-after EV-depl FBS. The sodium dodecyl-sulfate polyacrylamide gel electrophoresis (SDS-PAGE) gels are shown for each experiment, and the total protein amount was used for protein normalization. Pellets obtained after the 100,000 × g centrifugation of FBS was used as the control. $N = 2$. EV, extracellular vesicles; EV-depl, EV depleted; FBS, foetal bovine serum; HI, heat inactivation; S-EVs, small EVs.

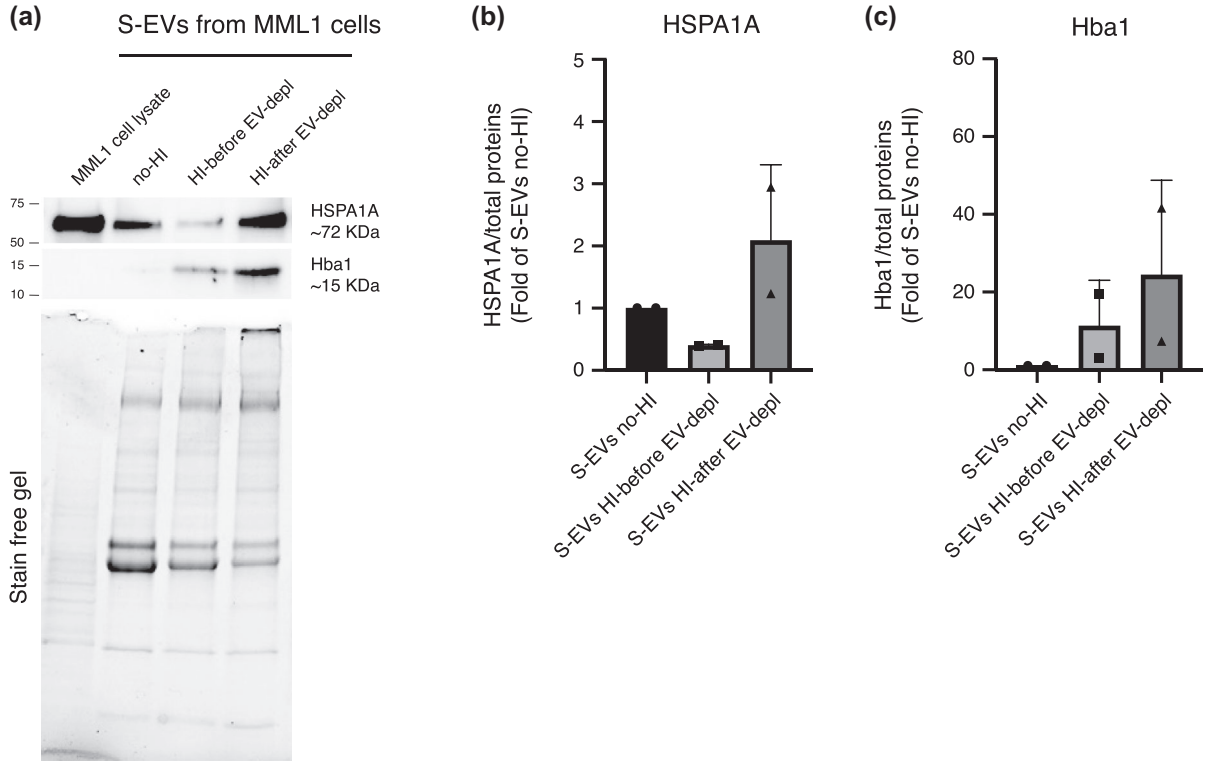

FIGURE 7 Bovine proteins can be detected in human cell-derived EVs. (a) Western blot of HSPA1A and Hba1 in S-EVs isolated from MML-1 cells cultured in media supplemented with no-HI FBS, HI-before EV-depl FBS, and HI-after EV-depl FBS. (b) Densitometric analysis of HSPA1A and (c) Hba1 in S-EVs isolated from MML-1 cells cultured in media supplemented with no-HI FBS, HI-before EV-depl FBS, and HI-after EV-depl FBS. The SDS-PAGE gels are shown for each experiment, and the total protein amount was used for protein normalization. MML-1 cell lysate was used as the control. $N = 2$. EV, extracellular vesicles; EV-depl, EV depleted; FBS, foetal bovine serum; HI, heat inactivation; S-EVs, small EVs.

To measure the possible impact of proteins enriched in S-EVs from HI-after EV-depl FBS on the analysis of proteins identified in cell-derived EVs, we compared our sample of interest with proteins listed in the online EV database Vesiclepedia (Kalra et al., 2012) (Figure S9). We found that the majority of the proteins enriched in S-EVs from HI-after EV-depl FBS versus no-HI FBS and versus HI-before EV-depl FBS were previously identified in human cell-derived EVs, thus suggesting that FBS proteins can be wrongly attributed to human cell-derived EVs.

4 | DISCUSSION

In this work, we demonstrated that heat inactivation of FBS (56°C for 30 min under agitation) prior to adding it to cell culture media impacts the purity of EVs isolated from cell cultures. We isolated L-EVs and S-EVs from three cell lines cultured in media supplemented with FBS that underwent no-HI, HI-before EV-depl and HI-after EV-depl, and we demonstrated that heat inactivated FBS after EV depletion by UC contaminated S-EV samples but not L-EV samples. Through proteomic analysis, we identified protein contaminants and found that some of the identified proteins could be mistakenly attributed to human cell-derived S-EVs.

As reported in our recent work (Urzì et al., 2022), although FBS is still the most common supplement for cell culture media, its use may become a disadvantage due to the presence of contaminants (endotoxins, viruses and mycoplasma) (Baker, 2016) and EVs that can end up in cell-derived EV samples (Théry et al., 2001). The most commonly used technique for FBS EV depletion (centrifugation at 100,000 × *g* for 18 h) (Théry et al., 2018) is unable to completely eliminate EVs from FBS as previously reported (Lehrich et al., 2018; Shelke et al., 2014) and confirmed in this study. Despite the efforts of the scientific community to standardize the protocols to reduce FBS-derived contaminants in cell-derived EV samples (Shelke et al., 2014), one aspect that has not be taken in consideration is the heat inactivation procedure.

Our results showed that FBS heat inactivation performed after EV depletion increases the protein contaminants. To confirm whether those protein contaminants could affect the purity of cell-derived EVs, three melanoma cell lines were cultured in media supplemented with no-HI FBS, HI-before EV-depl FBS and HI-after EV-depl FBS. Because some studies have demonstrated that heat inactivation of FBS can impair cell growth and phenotype (Bird & Owen, 1998; Eitan et al., 2015; Giard, 1987; Tonarova

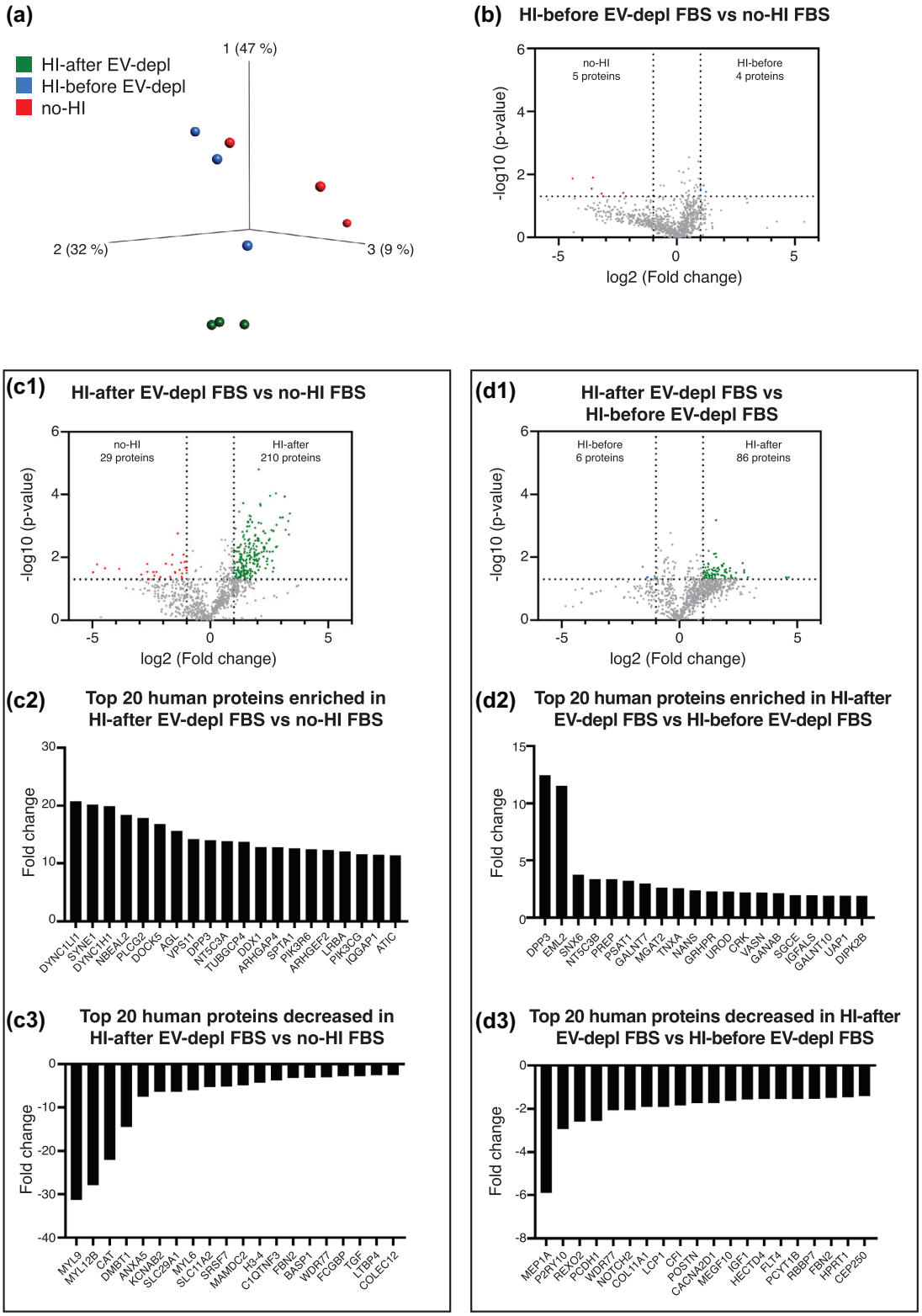

FIGURE 8 Analysis of S-EVs isolated from FBS compared to the human dataset. Quantitative proteomics (TMT) was used to determine the differences in the S-EVs isolated from no-HI FBS, HI-before EV-depl FBS, and HI-after EV-depl FBS, $N = 3$. (a) Principal component analysis illustrating the relation between S-EVs isolated from no-HI FBS (red), HI-before EV-depl FBS (blue), and HI-after EV-depl FBS (green). (b, c1 and d1) Volcano plots showing proteins with differential expression between S-EVs from no-HI FBS and HI-before EV-depl FBS (b), between S-EVs from HI-after EV-depl FBS and no-HI FBS (c1), and between S-EVs from HI-before EV-depl FBS and HI-after EV-depl FBS (d1). Grey dotted lines show p-value < 0.05 and two-fold change cut-offs. (c2–c3) The 20 most enriched (c2) and decreased (c3) bovine proteins in S-EVs isolated from HI-after EV-depl FBS versus no-HI FBS. (d2–d3) The 20 most enriched and decreased bovine proteins in S-EVs isolated from HI-after EV-depl FBS versus HI-before EV-depl FBS. $N = 3$. EV, extracellular vesicles; EV-depl, EV depleted; FBS, foetal bovine serum; HI, heat inactivation; S-EVs, small EVs.

et al., 2021), we first analysed the cell viability and morphology of melanoma cells maintained in media supplemented with FBS obtained following the three protocols. We performed the experiments on three different cell lines to extend the results to several *in vitro* models—MML-1 is a commercially available melanoma cell line, while UM22Bap1$^{+/+}$ and UM22Bap1$^{-/-}$ are genetically engineered patient-derived cells (Karlsson et al., 2020). While we did not observe any significant changes in cell viability, the growth of MML-1 cells in media with HI-before EV-depl FBS and HI-after EV-depl FBS was slightly reduced compared to media plus no-HI no-EV-depl FBS (Figure S4a). Previous studies demonstrated that heat-inactivated FBS (Bird & Owen, 1998; Tonarova et al., 2021) as well as FBS EV depletion (Ochieng et al., 2009) can affect cell metabolism and growth, and this could be the reason why MML-1 cell growth was reduced in media supplemented with HI-before EV-depl FBS and HI-after EV-depl FBS.

Given the observed increase in protein concentration of S-EV samples obtained from HI-after EV-depl FBS, quantitative mass spectrometry analysis was performed to identify the EV proteins that were differentially abundant in S-EVs from HI-after EV-depl FBS versus HI-before EV-depl FBS and no-HI FBS. To our knowledge, this is the first study that has investigated the protein content of FBS-derived EVs differently from previous works that have focused mainly on complete FBS and its effects on the secretome (Abramowicz et al., 2018; Nonnis et al., 2016; Shin et al., 2015, 2019). We found that proteins isolated from S-EVs derived from HI-after EV-depl FBS varied significantly from S-EVs derived from no-HI FBS and HI-after EV-depl FBS. The enrichment of HSP90, HSPA1A and Hba1 in S-EVs from HI-after EV-depl FBS was confirmed by western blot analysis. HSP90 is of high interest in the EV field because it is among the most enriched proteins in EVs, and it is considered an EV marker (Théry et al., 2018). Moreover, several studies demonstrated that HSP90-rich EVs play essential roles in cancer, including cell growth, survival, immune escape, migration, invasion and angiogenesis (Sager et al., 2022; Tang et al., 2019, 2022). HSPA1A, also known as HSP70, has been identified in EVs derived from human ovarian cancer cells (Klink et al., 2012), rat myometrial cells (Russell et al., 2021) and even lemon juice (Urzì et al., 2023), thus representing an established EV marker. Due to the homology of HSPA1A and Hba1 between humans and bovines, our results indicate that we cannot exclude that the enrichment observed in cell-derived EVs may be, at least partially, ascribable to FBS. On the other hand, Hba1 was previously found in microvesicles released by red blood cells (Thangaraju et al., 2020) and thus it was not surprising to find it in FBS-derived samples.

Although there are no studies in the literature that have directly compared the protein contents of FBS before and after heat inactivation, it is known that the proteome of cells cultured in media supplemented with heat-inactivated FBS can differ from the same cells grown in media supplemented with non-heat-inactivated FBS (Bruinink et al., 2004; Rahman et al., 2011), thus suggesting that the FBS protein content is affected by the heat inactivation procedure. Of note, it has previously been demonstrated that heat inactivation of human serum causes protein aggregation (Soltis et al., 1979) and that FBS heat inactivation causes the denaturation of the protein corona due to structural changes induced by the increased temperature, thus reducing the binding affinity of the serum proteins (Lesniak et al., 2010; Simon et al., 2018). Moreover, it has been recently shown that the interaction between plasma proteins and EVs may affect the EV corona composition (Tóth et al., 2021). These effects may explain the differences that we observed in the three conditions investigated (no-HI FBS, HI-before EV-depl FBS and HI-after EV-depl FBS) and FBS heat inactivation may increase protein stickiness, thus affecting the protein corona. Consequently, FBS proteins might precipitate and pellet differently during the UC process depending on the heat inactivation timing. Based on the results of these previous studies (Lesniak et al., 2010; Simon et al., 2018; Soltis et al., 1979; Tóth et al., 2021), future studies are needed to clarify the effect of heat inactivation on the FBS protein configuration and corona proteins.

The search for FBS-derived EV proteins in the human database identified several proteins that could be attributed to human origin. This result could be explained by the existing homology between the human and bovine species (Abdoli et al., 2018). Previous studies demonstrated that human antibodies can incorrectly recognize bovine proteins. In particular, Shelke et al. detected the presence of TSG101, CD81 and CD63 in EVs isolated from FBS using anti-human antibodies, thus highlighting the very high homology between humans and bovines (Shelke et al., 2014). Importantly, most of the proteins that were enriched in FBS-derived EVs from HI-after EV-depl FBS versus no-HI FBS and HI-before EV-depl FBS have been previously described in cell-derived EV proteomics studies (Gopal et al., 2015; Zhang et al., 2021). These could at least partly be due to FBS and mistakenly attributed to human cell line-derived EVs. Eight of these proteins were found in the top 100 proteins in Vesiclepedia (Kalra et al., 2012), which is the most commonly used database for studies on EV proteins. Previous studies, focused on bovine RNA contamination in EV samples, suggested using unconditioned media as the control with the aim to determine the "background" RNA levels to be subtracted from the RNA found in EV samples (Deutinger et al., 1988; Kamalov, 1989). Something similar could be done for proteomic analyses to avoid data misinterpretation.

The presence of bovine proteins in cell-derived S-EVs was confirmed through western blot and ELISA assays. Intriguingly, all the bovine proteins analysed (HSPA1A, Hba1 and CPN1) were previously identified in EVs. As mentioned above, HSPA1A is known to be enriched in EVs (Klink et al., 2012), Hba1c was identified in red blood cells derived EVs (Thangaraju et al., 2020) and CPN1 was previously described in EVs isolated from plasma (Bansal et al., 2020; Mao et al., 2021), thus taking into account the nature of our starting sample, their presence in S-EVs from FBS is not a surprise. The enrichment of HSPA1A and Hba1 in S-EVs isolated from HI-after EV-depl FBS compared to no-HI FBS and HI-after EV-depl FBS was also confirmed in S-EVs isolated from MML1 cells cultured in media supplemented with HI-after EV-depl FBS compared to the other two conditions. In line with these findings, bovine CPN1 protein levels were higher in S-EVs from cells cultured in media plus HI-after EV-depl FBS compared to no-HI FBS and HI-before EV-depl FBS (Figure S8a–c). Of note, Hba1 was not present in cell lysates, but it was

enriched in S-EVs isolated from cell supernatants containing HI-after EV-depl FBS (Figure 7a,c). Even if we cannot exclude that the Hba1 level in cell lysates is too low to be detectable by western blot, the Hba1 enrichment observed in S-EVs isolated from cell supernatants containing HI-after EV-depl FBS is a strong indication that the presence of Hba1 is due to the heat inactivation of FBS performed after EV depletion.

The detection of bovine proteins in human cell-derived S-EVs represents a clear proof that when the heat inactivation is performed, protein contaminants may end up in S-EV pellets. Differently from Hba1, HSPA1A was detected in MML-1 cell lysates (used as control, Figure 7a,b). The detection of HSPA1A in MML-1 cell lysates may be explained by species cross reactivity between humans and bovines.

Our results are strictly focused on the methodologies and proteomic analyses, and they shed light on the issues induced by the FBS heat inactivation process on cell-derived EVs. It is important to underline that we performed the protein measurement using Qubit assay. This type of quantification depends not only on the protein sequence, but it could be influenced by the changes in protein structure (Bocian et al., 2020), which could be induced by FBS heat inactivation. Future studies may help to explore the functional effects of the contaminates produced during the FBS heat inactivation and to define to what extent the effects of EVs on the recipient cells may be due to the FBS contaminants.

5 | CONCLUSION

In this study, we highlighted for the first time the contribution of FBS in EV samples linked to the timing of FBS heat inactivation. We demonstrated that heat inactivation of FBS can reduce EV purity, increase the amount of cell-derived EV proteins, and confound subsequent proteomic analysis. Moreover, we demonstrated that the heat inactivation performed after EV depletion induces contamination of cell-derived EV by proteins of bovine origin. We strongly suggest specifying in all EV studies whether the heat inactivation of FBS is performed, and we recommend either avoiding heat inactivation or, if it is necessary, to do it prior to EV depletion.

AUTHOR CONTRIBUTIONS

Ornella Urzì: Data curation; formal analysis; methodology; writing—original draft; writing—review and editing. **Markus Bergqvist**: Data curation; methodology; validation. **Cecilia Lässer**: Formal analysis; writing—review and editing. **Marta Moschetti**: Investigation; methodology. **Junko Johansson**: Methodology. **Daniele D´Arrigo**: Methodology. **Roger Olofsson Bagge**: Funding acquisition; resources; writing—review and editing. **Rossella Crescitelli**: Conceptualization; data curation; formal analysis; funding acquisition; investigation; methodology; resources; supervision; validation; visualization; writing—original draft; writing—review and editing.

ACKNOWLEDGEMENTS

The authors acknowledge Jan Lötvall for giving conceptual advice and for the assistance in interpreting the data. We acknowledge the Centre for Cellular Imaging (CCI) at University of Gothenburg and the National Microscopy Infrastructure, NMI (VR-RFI 2019-00217) for providing assistance in microscopy. For proteomic analysis we thank Annika Thorsell at the Proteomics Core Facility at Sahlgrenska Academy, University of Gothenburg. The proteomic analysis was performed with financial support from SciLifeLab and BioMS. We thank Jonas Nilsson and Lisa Nilsson for kindly sharing the UM22Bap1$^{+/+}$ and UM22Bap1$^{-/-}$ cell lines. The authors acknowledge Roberto Cattaneo for his assistance with graphic design. Major funding was from the Swedish Research Council, Swedish Cancer Foundation, the Knut and Alice Wallenberg Foundation, and the Wallenberg Centre for Molecular and Translational Medicine, University of Gothenburg, Sweden. Rossella Crescitelli was also supported by the Assar Gabrielsson's foundation (Grant # FB21-113), the Wilhelm och Martina Lundgrens Vetenskapsfond (2023-SA-4142), the Anna Lisa and Björnssons foundation and the Serena Ehrenströms fond för Kräftsjukdomarnas. Open Access funding was provided by the University of Gothenburg. OU was a PhD student in "Biomedicina, Neuroscienze e Diagnostica Avanzata", XXXV ciclo, University of Palermo. MM is a PhD student in "Oncologia e Chirurgia Sperimentale", XXXIV ciclo, University of Palermo when most of the experiments have been performed.

CONFLICT OF INTEREST STATEMENT

RC and CL have developed multiple EV-associated patents for putative clinical utilization and they own equity in Exocure Sweden AB. ROB has received institutional research grants from Bristol-Myers Squibb (BMS), Endomagnetics Ltd (Endomag), and SkyLineDx, speaker honoraria from Roche, Pfizer, and Pierre-Fabre, and has served on advisory boards for Amgen, BD/BARD, Bristol-Myers Squibb (BMS), Merck Sharp, & Dohme (MSD), Novartis, Roche, and Sanofi Genzyme and is a shareholder in SATMEG Ventures AB.

ORCID

Rossella Crescitelli https://orcid.org/0000-0002-1714-3169

REFERENCES

Abdoli, R., Zamani, P., & Ghasemi, M. (2018). Genetic similarities and phylogenetic analysis of human and farm animal species based on mitogenomic nucleotide sequences. *Meta Gene*, *15*, 23–26.

Abramowicz, A., Marczak, L., Wojakowska, A., Zapotoczny, S., Whiteside, T. L., Widlak, P., & Pietrowska, M. (2018). Harmonization of exosome isolation from culture supernatants for optimized proteomics analysis. *PLoS ONE*, *13*, e0205496.

Aqrawi, L. A., Aqrawi, L. A., Galtung, H. K., Vestad, B., Øvstebø, R., Thiede, B., Rusthen, S., Young, A., Guerreiro, E. M., Utheim, T. P., Chen, X., Utheim, Ø. A., Palm, Ø., & Jensen, J. L. (2017). Identification of potential saliva and tear biomarkers in primary Sjögren's syndrome, utilising the extraction of extracellular vesicles and proteomics analysis. *Arthritis Research & Therapy*, *19*, 14.

Aswad, H., Jalabert, A., & Rome, S. (2016). Depleting extracellular vesicles from fetal bovine serum alters proliferation and differentiation of skeletal muscle cells in vitro. *BMC Biotechnology [Electronic Resource]*, *16*, 32.

Molenaar-de Backer, M. W. A., Gitz, E., Dieker, M., Doodeman, P., & Ten Brinke, A. (2021). Performance of monocyte activation test supplemented with human serum compared to fetal bovine serum. *Altex*, *38*, 307–315.

Baker, M. (2016). Reproducibility: Respect your cells! *Nature*, *537*, 433–435.

Bansal, S., McGilvrey, M., Garcia-Mansfield, K., Sharma, R., Bremner, R. M., Smith, M. A., Hachem, R., Pirrotte, P., & Mohanakumar, T. (2020). Global proteomics analysis of circulating extracellular vesicles isolated from lung transplant recipients. *ACS Omega*, *5*, 14360–14369.

Bird, M., & Owen, A. (1998). Neurite outgrowth-regulating properties of GABA and the effect of serum on mouse spinal cord neurons in culture. *Journal of Anatomy*, *193*(Pt 4), 503–508.

Bocian, A., Sławek, S., Jaromin, M., Hus, K. K., Buczkowicz, J., Łysiak, D., Petrílla, V., Petrillova, M., & Legáth, J. (2020). Comparison of methods for measuring protein concentration in venom samples. *Animals (Basel)*, 10.

Bruinink, A., Tobler, U., Hälg, M., & Grünert, J. (2004). Effects of serum and serum heat-inactivation on human bone derived osteoblast progenitor cells. *Journal of Materials Science. Materials in Medicine*, *15*, 497–501.

Bryan, N., Andrews, K. D., Loughran, M. J., Rhodes, N. P., & Hunt, J. A. (2011). Elucidating the contribution of the elemental composition of fetal calf serum to antigenic expression of primary human umbilical-vein endothelial cells in vitro. *Bioscience Reports*, *31*, 199–210.

Caby, M. P., Lankar, D., Vincendeau-Scherrer, C., Raposo, G., & Bonnerot, C. (2005). Exosomal-like vesicles are present in human blood plasma. *International Immunology*, *17*, 879–887.

Crescitelli, R., Lässer, C., Jang, S. C., Cvjetkovic, A., Malmhäll, C., Karimi, N., Höög, J. L., Johansson, I., Fuchs, J., Thorsell, A., Gho, Y. S., Olofsson Bagge, R., & Lötvall, J. (2020). Subpopulations of extracellular vesicles from human metastatic melanoma tissue identified by quantitative proteomics after optimized isolation. *Journal of Extracellular Vesicles*, *9*, 1722433.

Crescitelli, R., Lässer, C., & Lötvall, J. (2021). Isolation and characterization of extracellular vesicle subpopulations from tissues. *Nature Protocols*, *16*, 1548–1580.

Crescitelli, R., Lässer, C., Szabo, T. G., Kittel, A., Eldh, M., Dianzani, I., Buzás, E. I., & Lötvall, J. (2013). Distinct RNA profiles in subpopulations of extracellular vesicles: apoptotic bodies, microvesicles and exosomes. *Journal of Extracellular Vesicles*, *2*(1), 20677.

Deutinger, J., Rudelstorfer, R., & Bernaschek, G. (1988). Vaginosonographic velocimetry of both main uterine arteries by visual vessel recognition and pulsed Doppler method during pregnancy. *American Journal of Obstetrics and Gynecology*, *159*, 1072–1076.

Doyle, L. M., & Wang, M. Z. (2019). Overview of extracellular vesicles, their origin, composition, purpose, and methods for exosome isolation and analysis. *Cells*, *8*.

Eitan, E., Zhang, S., Witwer, K. W., & Mattson, M. P. (2015). Extracellular vesicle-depleted fetal bovine and human sera have reduced capacity to support cell growth. *Journal of Extracellular Vesicles*, *4*, 26373.

Giard, D. J. (1987). Routine heat inactivation of serum reduces its capacity to promote cell attachment. *In Vitro Cellular & Developmental Biology*, *23*, 691–697.

Gopal, S. K., Greening, D. W., Mathias, R. A., Ji, H., Rai, A., Chen, M., Zhu, H. J., & Simpson, R. J. (2015). YBX1/YB-1 induces partial EMT and tumourigenicity through secretion of angiogenic factors into the extracellular microenvironment. *Oncotarget*, *6*, 13718–13730.

Gstraunthaler, G. (2003). Alternatives to the use of fetal bovine serum: serum-free cell culture. *Altex*, *20*, 275–281.

Haghighitalab, A., Matin, M. M., Khakrah, F., Asoodeh, A., & Bahrami, A. R. (2020). Cost-effective strategies for depletion of endogenous extracellular vesicles from fetal bovine serum. *Journal of Cell and Molecular Research*, *11*, 42–54.

Harding, C., Heuser, J., & Stahl, P. (1983). Receptor-mediated endocytosis of transferrin and recycling of the transferrin receptor in rat reticulocytes. *The Journal of cell Biology*, *97*, 329–339.

Herrmann, I. K., Wood, M. J. A., & Fuhrmann, G. (2021). Extracellular vesicles as a next-generation drug delivery platform. *Nature Nanotechnology*, *16*, 748–759.

Jochems, C. E., van der Valk, J. B., Stafleu, F. R., & Baumans, V. (2002). The use of fetal bovine serum: Ethical or scientific problem? *Alternatives to Laboratory Animals*, *30*, 219–227.

Kalra, H., Simpson, R. J., Ji, H., Aikawa, E., Altevogt, P., Askenase, P., Bond, V. C., Borràs, F. E., Breakefield, X., Budnik, V., Buzas, E., Camussi, G., Clayton, A., Cocucci, E., Falcon-Perez, J. M., Gabrielsson, S., Gho, Y. S., Gupta, D., Harsha, H. C., … Mathivanan, S. (2012). Vesiclepedia: A compendium for extracellular vesicles with continuous community annotation. *PLoS Biology*, *10*, e1001450.

Kamalov, I. I. (1989). Comparative clinico-roentgenological characteristics of degenerative-dystrophic changes in various segments of the spine. *Zhurnal Nevropatologii I Psikhiatrii Imeni S.S. Korsakova (Moscow, Russia: 1952)*, *89*, 28–31.

Karlsson, J., Nilsson, L. M., Mitra, S., Alsén, S., Shelke, G. V., Sah, V. R., Forsberg, E. M. V., Stierner, U., All-Eriksson, C., Einarsdottir, B., Jespersen, H., Ny, L., Lindnér, P., Larsson, E., Olofsson Bagge, R., & Nilsson, J. A. (2020). Molecular profiling of driver events in metastatic uveal melanoma. *Nature Communications*, *11*, 1894.

Klink, M., Nowak, M., Kielbik, M., Bednarska, K., Blus, E., Szpakowski, M., Szyllo, K., & Sulowska, Z. (2012). The interaction of HspA1A with TLR2 and TLR4 in the response of neutrophils induced by ovarian cancer cells in vitro. *Cell Stress & Chaperones*, *17*, 661–674.

Kornilov, R., Puhka, M., Mannerström, B., Hiidenmaa, H., Peltoniemi, H., Siljander, P., Seppänen-Kaijansinkko, R., & Kaur, S. (2018). Efficient ultrafiltration-based protocol to deplete extracellular vesicles from fetal bovine serum. *Journal of Extracellular Vesicles*, *7*, 1422674.

Lehrich, B. M., Liang, Y., Khosravi, P., Federoff, H. J., & Fiandaca, M. S. (2018). Fetal bovine serum-derived extracellular vesicles persist within vesicle-depleted culture media. *International Journal of Molecular Sciences*, *19*(11), 3538.

Lesniak, A., Campbell, A., Monopoli, M. P., Lynch, I., Salvati, A., & Dawson, K. A. (2010). Serum heat inactivation affects protein corona composition and nanoparticle uptake. *Biomaterials*, *31*, 9511–9518.

Mannerström, B., Paananen, R. O., Abu-Shahba, A. G., Moilanen, J., Seppänen-Kaijansinkko, R., & Kaur, S. (2019). Extracellular small non-coding RNA contaminants in fetal bovine serum and serum-free media. *Scientific Reports*, *9*, 5538.

Mao, K., Tan, Q., Ma, Y., Wang, S., Zhong, H., Liao, Y., Huang, Q., Xiao, W., Xia, H., Tan, X., Luo, P., Xu, J., Long, D., & Jin, Y. (2021). Proteomics of extracellular vesicles in plasma reveals the characteristics and residual traces of COVID-19 patients without underlying diseases after 3 months of recovery. *Cell Death & Disease*, *12*, 541.

Nonnis, S., Maffioli, E., Zanotti, L., Santagata, F., Negri, A., Viola, A., Elliman, S., & Tedeschi, G. (2016). Effect of fetal bovine serum in culture media on MS analysis of mesenchymal stromal cells secretome. *EuPA Open Proteom*, *10*, 28–30.

Norman, M., Ter-Ovanesyan, D., Trieu, W., Lazarovits, R., Kowal, E. J., Lee, J. H., Chen-Plotkin, A. S., Regev, A., Church, G. M., & Walt, D. R. (2021). L1CAM is not associated with extracellular vesicles in human cerebrospinal fluid or plasma. *Nature Methods*, *18*, 631–634.

Ochieng, J., Pratap, S., Khatua, A. K., & Sakwe, A. M. (2009). Anchorage-independent growth of breast carcinoma cells is mediated by serum exosomes. *Experimental Cell Research*, *315*, 1875–1888.

Pan, B. T., & Johnstone, R. M. (1983). Fate of the transferrin receptor during maturation of sheep reticulocytes in vitro: Selective externalization of the receptor. *Cell*, *33*, 967–978.

Perez-Riverol, Y., Bai, J., Bandla, C., García-Seisdedos, D., Hewapathirana, S., Kamatchinathan, S., Kundu, D. J., Prakash, A., Frericks-Zipper, A., Eisenacher, M., Walzer, M., Wang, S., Brazma, A., & Vizcaíno, J. A. (2022). The PRIDE database resources in 2022: A hub for mass spectrometry-based proteomics evidences. *Nucleic Acids Research*, *50*, D543–d552.

Pham, C. V., Midge, S., Barua, H., Zhang, Y., Nguyen, T. N. G., Barrero, R. A., Duan, A., Yin, W., Jiang, G., Hou, Y., Zhou, S., Wang, Y., Xie, X., Tran, P. H. L., Xiang, D., & Duan, W. (2021). Bovine extracellular vesicles contaminate human extracellular vesicles produced in cell culture conditioned medium when 'exosome-depleted serum' is utilised. *Archives of Biochemistry and Biophysics*, *708*, 108963.

Pisitkun, T., Shen, R. F., & Knepper, M. A. (2004). Identification and proteomic profiling of exosomes in human urine. *PNAS*, *101*, 13368–13373.

Pucci, M., Raimondo, S., Urzì, O., Moschetti, M., Di Bella, M. A., Conigliaro, A., Caccamo, N., La Manna, M. P., Fontana, S., & Alessandro, R. (2021). Tumor-derived small extracellular vesicles induce pro-inflammatory cytokine expression and PD-L1 regulation in M0 macrophages via IL-6/STAT3 and TLR4 signaling pathways. *International Journal of Molecular Sciences*, *22*(22), 12118.

Rahman, H., Qasim, M., Schultze, F. C., Oellerich, M., & A, R. A. (2011). Fetal calf serum heat inactivation and lipopolysaccharide contamination influence the human T lymphoblast proteome and phosphoproteome. *Proteome Science*, *9*, 71.

Raposo, G., Nijman, H. W., Stoorvogel, W., Liejendekker, R., Harding, C. V., Melief, C. J., & Geuze, H. J. (1996). B lymphocytes secrete antigen-presenting vesicles. *The Journal of Experimental Medicine*, *183*, 1161–1172.

Russell, M. F., Bailey, G. C., Miskiewicz, E. I., & MacPhee, D. J. (2021). Inducible heat shock protein A1A (HSPA1A) is markedly expressed in rat myometrium by labour and secreted via myometrial cell-derived extracellular vesicles. *Reproduction, Fertility, and Development*, *33*, 279–290.

Sager, R. A., Khan, F., Toneatto, L., Votra, S. D., Backe, S. J., Woodford, M. R., Mollapour, M., & Bourboulia, D. (2022). Targeting extracellular Hsp90: A unique frontier against cancer. *Frontiers in Molecular Biosciences*, *9*, 982593.

Shelke, G. V., Lässer, C., Gho, Y. S., & Lötvall, J. (2014). Importance of exosome depletion protocols to eliminate functional and RNA-containing extracellular vesicles from fetal bovine serum. *Journal of Extracellular Vesicles*, *3*(1), 24783.

Shen, Y., Halperin, J. A., Benzaquen, L., & Lee, C. M. (1997). Characterization of neuronal cell death induced by complement activation. *Brain Research Brain Research Protocols*, *1*, 186–194.

Shin, J., Kim, G., Kabir, M. H., Park, S. J., Lee, S. T., & Lee, C. (2015). Use of composite protein database including search result sequences for mass spectrometric analysis of cell secretome. *PLoS ONE*, *10*, e0121692.

Shin, J., Kwon, Y., Lee, S., Na, S., Hong, E. Y., Ju, S., Jung, H. G., Kaushal, P., Shin, S., Back, J. H., Choi, S. Y., Kim, E. H., Lee, S. J., Park, Y. E., Ahn, H. S., Ahn, Y., Kabir, M. H., Park, S. J., Yang, W. S., … Lee, C. (2019). Common repository of FBS proteins (cRFP) to be added to a search database for mass spectrometric analysis of cell secretome. *Journal of Proteome Research*, *18*, 3800–3806.

Shoffner, J. M., & Wallace, D. C. (1992). Mitochondrial genetics: Principles and practice. *American Journal of Human Genetics*, *51*, 1179–1186.

Simon, J., Müller, J., Ghazaryan, A., Morsbach, S., Mailänder, V., & Landfester, K. (2018). Protein denaturation caused by heat inactivation detrimentally affects biomolecular corona formation and cellular uptake. *Nanoscale*, *10*, 21096–21105.

Słomka, A., Urban, S. K., Lukacs-Kornek, V., Żekanowska, E., & Kornek, M. (2018). Large extracellular vesicles: have we found the holy grail of inflammation? *Frontiers in Immunology*, *9*, 2723.

Soltis, R. D., Hasz, D., Morris, M. J., & Wilson, I. D. (1979). The effect of heat inactivation of serum on aggregation of immunoglobulins. *Immunology*, *36*, 37–45.

Svennerholm, K., Park, K. S., Wikström, J., Lässer, C., Crescitelli, R., Shelke, G. V., Jang, S. C., Suzuki, S., Bandeira, E., Olofsson, C. S., & Lötvall, J. (2017). Escherichia coli outer membrane vesicles can contribute to sepsis induced cardiac dysfunction. *Scientific Reports*, *7*, 17434.

Tang, H., Zhou, X., Zhao, X., Luo, X., Luo, T., Chen, Y., Liang, W., Jiang, E., Liu, K., Shao, Z., & Shang, Z. (2022). HSP90/IKK-rich small extracellular vesicles activate pro-angiogenic melanoma-associated fibroblasts via the NF-κB/CXCL1 axis. *Cancer Science*, *113*, 1168–1181.

Tang, X., Chang, C., Guo, J., Lincoln, V., Liang, C., Chen, M., Woodley, D. T., & Li, W. (2019). Tumour-secreted Hsp90α on external surface of exosomes mediates tumour - stromal cell communication via autocrine and paracrine mechanisms. *Scientific Reports*, *9*, 15108.

Thangaraju, K., Neerukonda, S. N., Katneni, U., & Buehler, P. W. (2020). Extracellular vesicles from red blood cells and their evolving roles in health, coagulopathy and therapy. *International Journal of Molecular Sciences*, *22*(1), 153.

Thery, C., Boussac, M., Véron, P., Ricciardi-Castagnoli, P., Raposo, G., Garin, J., & Amigorena, S. (2001). Proteomic analysis of dendritic cell-derived exosomes: a secreted subcellular compartment distinct from apoptotic vesicles. *Journal of Immunology*, *166*, 7309–7318.

Théry, C., Amigorena, S., Raposo, G., & Clayton, A. (2006). Isolation and characterization of exosomes from cell culture supernatants and biological fluids. *Current Protocols in Cell Biology*, *Chapter 3*, Unit 3.22.

Théry, C., Witwer, K. W., Aikawa, E., Alcaraz, M. J., Anderson, J. D., Andriantsitohaina, R., Antoniou, A., Arab, T., Archer, F., Atkin-Smith, G. K., Ayre, D. C., Bach, J. M., Bachurski, D., Baharvand, H., Balaj, L., Baldacchino, S., Bauer, N. N., Baxter, A. A., Bebawy, M., … Zuba-Surma, E. K. (2018). Minimal information for studies of extracellular vesicles 2018 (MISEV2018): A position statement of the international society for extracellular vesicles and update of the MISEV2014 guidelines. *Journal of Extracellular Vesicles*, *7*, 1535750.

Tonarova, P., Lochovska, K., Pytlik, R., & Hubalek Kalbacova, M. (2021). The impact of various culture conditions on human mesenchymal stromal cells metabolism. *Stem Cells Int*, *2021*, 6659244.

Tóth, E., Turiák, L., Visnovitz, T., Cserép, C., Mázló, A., Sódar, B. W., Försönits, A. I., Petővári, G., Sebestyén, A., Komlósi, Z., Drahos, L., Kittel, Á., Nagy, G., Bácsi, A., Dénes, Á., Gho, Y. S., Szabó-Taylor, K. É., & Buzás, E. I. (2021). Formation of a protein corona on the surface of extracellular vesicles in blood plasma. *Journal of Extracellular Vesicles*, *10*, e12140.

Triglia, R. P., & Linscott, W. D. (1980). Titers of nine complement components, conglutinin and C3b-inactivator in adult and fetal bovine sera. *Molecular Immunology*, *17*, 741–748.

Urzì, O., Bagge, R. O., & Crescitelli, R. (2022). The dark side of foetal bovine serum in extracellular vesicle studies. *Journal of Extracellular Vesicles*, *11*, e12271.

Urzì, O., Cafora, M., Ganji, N. R., Tinnirello, V., Gasparro, R., Raccosta, S., Martinez, Z. A., Baetens, T., Beghein, E., Bertier, L., Berx, G., Boere, J., Boukouris, S., Bremer, M., Buschmann, D., Byrd, J. B., Casert, C., Cheng, L., Cmoch, A., … Hendrix, A. (2023). Lemon-derived nanovesicles achieve antioxidant and anti-inflammatory effects activating the AhR/Nrf2 signaling pathway. *Iscience*, *26*, 107041.

Van Deun, J., Mestdagh, P., Agostinis, P., Akay, Ö., Anand, S., Anckaert, J., Martinez, Z. A., Baetens, T., Beghein, E., Bertier, L., Berx, G., Boere, J., Boukouris, S., Bremer, M., Buschmann, D., Byrd, J. B., Casert, C., Cheng, L., Cmoch, A., … Hendrix, A. (2017). EV-TRACK: transparent reporting and centralizing knowledge in extracellular vesicle research. *Nature Methods*, *14*, 228–232.

van Niel, G., D'Angelo, G., & Raposo, G. (2018). Shedding light on the cell biology of extracellular vesicles. *Nature Reviews Molecular Cell Biology*, *19*, 213–228.

Wang, F., Cerione, R. A., & Antonyak, M. A. (2021). Isolation and characterization of extracellular vesicles produced by cell lines. *STAR Protocols*, *2*, 100295.

Wiśniewski, J. R., Zougman, A., Nagaraj, N., & Mann, M. (2009). Universal sample preparation method for proteome analysis. *Nature Methods*, *6*, 359–362.

Xu, R., Greening, D. W., Zhu, H. J., Takahashi, N., & Simpson, R. J. (2016). Extracellular vesicle isolation and characterization: Toward clinical application. *Journal of Clinical Investigation*, *126*, 1152–1162.

Yáñez-Mó, M., Yáñez-Mó, M., Siljander, P. R. M., Andreu, Z., Bedina Zavec, A., Borràs, F. E., Buzas, E. I., Buzas, K., Casal, E., Cappello, F., Carvalho, J., Colás, E., Cordeiro-da Silva, A., Fais, S., Falcon-Perez, J. M., Ghobrial, I. M., Giebel, B., Gimona, M., Graner, M., … Gursel, I. (2015). Biological properties of extracellular vesicles and their physiological functions. *Journal of Extracellular Vesicles*, *4*, 27066.

Yekula, A., Minciacchi, V. R., Morello, M., Shao, H., Park, Y., Zhang, X., Muralidharan, K., Freeman, M. R., Weissleder, R., Lee, H., Carter, B., Breakefield, X. O., Di Vizio, D., & Balaj, L. (2020). Large and small extracellular vesicles released by glioma cells in vitro and in vivo. *Journal of Extracellular Vesicles*, *9*, 1689784.

Yin, Y., Liu, B., Cao, Y., Yao, S., Liu, Y., Jin, G., Qin, Y., Chen, Y., Cui, K., Zhou, L., Bian, Z., Fei, B., Huang, S., & Huang, Z. (2020). Colorectal cancer-derived small extracellular vesicles promote tumor immune evasion by upregulating PD-L1 expression in tumor-associated macrophages. *Advance Science (Weinh)*, *9*, 2102620.

Zhang, M., Xie, Y., Li, S., Ye, X., Jiang, Y., Tang, L., & Wang, J. (2021). Proteomics analysis of exosomes from patients with active tuberculosis reveals infection profiles and potential biomarkers. *Frontiers in Microbiology*, *12*, 800807.

SUPPORTING INFORMATION

Additional supporting information can be found online in the Supporting Information section at the end of this article.

How to cite this article: Urzì, O., Bergqvist, M., Lässer, C., Moschetti, M., Johansson, J., D´Arrigo, D., Olofsson Bagge, R., & Crescitelli, R. (2024). Heat inactivation of foetal bovine serum performed after EV-depletion influences the proteome of cell-derived extracellular vesicles. *Journal of Extracellular Vesicles*, *13*, e12408. https://doi.org/10.1002/jev2.12408